Agricultural and Forest Meteorology 149 (2009) 2022–2039

Contents lists available at ScienceDirect

Agricultural and Forest Meteorology

journal homepage: www.elsevier.com/locate/agrformet

Interannual variation in net ecosystem productivity of Canadian forests as affected by regional weather patterns – A Fluxnet-Canada synthesis

R.F. Grant [a,*], A.G. Barr [b], T.A. Black [c], H.A. Margolis [d], A.L. Dunn [e], J. Metsaranta [f], S. Wang [g], J.H. McCaughey [h], C.A. Bourque [i]

[a] Department of Renewable Resources, University of Alberta, Edmonton, AB, Canada T6G 2E3
[b] Climate Research Branch, Meteorological Service of Canada, Saskatoon, SK, Canada S7N 3H5
[c] Department of Soil Science, University of British Columbia, Vancouver, BC, Canada V6T 1Z4
[d] Faculté de Foresterie et de Géomatique, Pavillon Abitibi-Price, Université Laval, Québec, Québec, Canada G1K 7P4
[e] Department of Physical and Earth Sciences, Worcester State College, Worcester, MA 01602, United States
[f] Canadian Forest Service, Natural Resources Canada, Victoria, BC, Canada V8Z 1M5
[g] Canada Centre for Remote Sensing, Natural Resources Canada, Ottawa, ON, Canada K1A 0E7
[h] Department of Geography, Queen's University, Kingston, Ontario, K7L 3N6 Canada
[i] Faculty of Forestry and Environmental Management, University of New Brunswick, Fredericton, New Brunswick, E3B 6C2 Canada

ARTICLE INFO

Article history:
Received 12 March 2009
Received in revised form 27 June 2009
Accepted 17 July 2009

Keywords:
Net ecosystem productivity
Modelling
Ecosys
Climate
Eddy covariance
NDVI

ABSTRACT

Large-scale weather events such as the El Niño Southern Oscillation (ENSO), Pacific Decadal Oscillation (PDO), and droughts are known to cause substantial interannual variation in the net ecosystem productivity (NEP) of tropical, temperate and boreal forests. Hypotheses for the impacts on NEP of changes in air temperature (T_a) and precipitation associated with these events were tested at diurnal, seasonal and annual time scales using the terrestrial ecosystem model *ecosys* with measurements of CO_2 and energy exchange from 1998 to 2006 at eddy covariance (EC) flux towers along a transcontinental transect of forest stands in the Fluxnet-Canada Research Network (FCRN).[1] These tests were supported at seasonal time scales by remotely-sensed vegetation indices, and at decadal time scales by wood growth increments from tree-ring and inventory studies. Collectively, results from this testing indicate that large-scale weather events during the study period caused spatially coherent changes in NEP, although these changes may vary with climate zone, species and topography. High T_a episodes, such as occurred with greater frequency during ENSO/PDO events, adversely affected diurnal CO_2 exchange of temperate and boreal conifers, but had little effect on that of a boreal deciduous forest. These contrasting responses of CO_2 exchange to T_a were attributed in the model to greater xylem resistance to water uptake in coniferous *vs.* deciduous trees. Sustained warming such as occurred during ENSO/PDO events extended the period of net C uptake and thus raised annual NEP at boreal coniferous and deciduous sites, but did not do so at a temperate coniferous site where annual NEP was reduced. However the rise in NEP of boreal conifers with warming was partially offset by the adverse effects of high T_a on diurnal CO_2 exchange, so that the rise in NEP with warming remained smaller than that at a boreal deciduous site. A 3-year drought during the study period adversely affected annual NEP of well-drained boreal deciduous forests but did not affect that of poorly-drained boreal conifers. This lack of effect was attributed in the model to low coniferous evapotranspiration rates and to subsurface water recharge. Drought effects on NEP were therefore largely determined by topography. These contrasting responses of different forest stands to warming and drought indicate divergent changes in forest growth with interannual changes in weather. Such divergent changes are consistent with the complex changes in forest NDVI and net C uptake observed over time in several large-scale remote-sensing studies.
© 2009 Elsevier B.V. All rights reserved.

1. Introduction

Large-scale weather patterns are known to cause substantial interannual variation in the net ecosystem productivity (NEP) of tropical, temperate and boreal forests. In tropical regions, droughts during El Niño Southern Oscillations (ENSO) hasten tree mortality and so reduce NEP as derived from extensive biometric measurements of rainforests (Clark, 2004; Saleska et al., 2003). In coastal temperate regions of western North America, high air temperatures (T_a) during an ENSO event reduced annual NEP as derived from eddy covariance (EC) measurements over a Douglas-fir stand in British Columbia (Morgenstern et al., 2004). Conversely, La Niña

* Corresponding author. Tel.: +1 780 492 6609; fax: +1 780 492 1767.
E-mail address: robert.grant@ales.ualberta.ca (R.F. Grant).
[1] Now the Canada Carbon Project.

0168-1923/$ – see front matter © 2009 Elsevier B.V. All rights reserved.
doi:10.1016/j.agrformet.2009.07.010

events were linked to lower T_a and excess rainfall (Shabbar and Skinner, 2004) that raised NEP of Douglas-fir (Morgenstern et al., 2004). Further north in the Gulf of Alaska, warmer conditions coinciding with positive phases of the Pacific Decadal Oscillation (PDO) were associated with increased radial growth as derived from tree ring chronologies of mountain hemlock and Sitka spruce (D'Arrigo et al., 2001).

In mid-continental regions of boreal North America, positive phases of the ENSO and PDO have been associated with warmer and drier winters (Bonsal et al., 2001), lower stream flows (Bonsal and Shabbar, 2008) and increased fire frequency (Fauria and Johnson, 2008). More persistent North Pacific SST anomalies, largely driven by PDO, ENSO and their interactions (Shabbar and Skinner, 2004), have been associated with summer droughts (Bonsal et al., 1993) that reduced forest productivity in Alberta, Saskatchewan and Manitoba (Hogg et al., 2008), and increased fire frequency as far east as northern Ontario and Quebec (Le Goff et al., 2007; Skinner et al., 2006). Recent evidence suggests that teleconnections between SST anomalies and continental patterns of temperature and precipitation may be changing (Bonsal and Wheaton, 2005).

These weather patterns overlay a longer-term warming trend thought to be caused by rising atmospheric CO_2 concentrations (C_a) which is causing general increases in net primary productivity (NPP) (Nemani et al., 2003) and NEP (Nabuurs et al., 2002; Rosenzweig et al., 2007) of temperate and boreal forests. These increases may be driven by an extension of the growing season of up to 2 weeks during the past 50 years in mid- and high northern latitudes, apparent in remotely-sensed vegetation indices (NDVI) (Myneni et al., 1997; Zhou et al., 2001) and in seasonal trends of C_a (Keeling et al., 1996). Growing season lengths estimated from NDVI in boreal coniferous forests have been positively correlated with C net uptake duration, and thereby with NEP (Churkina et al., 2005). However rises in NDVI and NPP with autumn warming may be offset by greater rises in heterotrophic respiration (R_h), causing earlier declines in late-season NEP (Piao et al., 2008). Long-term warming may adversely affect NEP of forests in tropical regions (Clark et al., 2003) or those near their upper limit of thermal adaptation (Jump et al., 2006).

The effects of large-scale weather patterns on NEP of temperate and boreal forests are caused by interannual variation in T_a and precipitation. EC measurements have shown that NEP of both coniferous and deciduous forests is raised by early spring warming (Arain et al., 2002; Grant et al., 2008), and that NEP of coniferous forests is reduced by hot summers (Griffis et al., 2003), often associated with positive PDO. These reductions in conifer NEP have been shown to be caused by concurrent declines in gross primary productivity (GPP) and rises in ecosystem respiration (R_e) under higher T_a (Grant et al., 2008; Griffis et al., 2003; Morgenstern et al., 2004). Similarly, tree-ring analyses have shown that growth of white spruce in Alaska responded positively to warmer springs and negatively to warmer summers (Barber et al., 2000; Wilmking et al., 2004), and that growth of black spruce in Alberta and Saskatchewan was negatively correlated with summer T_a (Dang and Lieffers, 1989; Brooks et al., 1998). Tree-ring studies in jack pine have also shown positive correlations of growth with spring T_a (Brooks et al., 1998) and precipitation (Larsen and MacDonald, 1995; Brooks et al., 1998; Savva et al., 2008), and negative correlations of growth with summer T_a (Larsen and MacDonald, 1995), because warming may exacerbate summer droughts (Savva et al., 2008). These findings are consistent with those from remote sensing studies in which the apparent decoupling of warming and forest growth during summer has been attributed to possible drought stress, nutrient limitation, insect and disease damage, and changes in resource allocation (Goetz et al., 2005).

Primary productivity of boreal deciduous forests is less sensitive to high T_a but more sensitive to low summer precipitation than is that of coniferous forests (Kljun et al., 2007) because their more rapid transpiration rates hasten the onset of soil water deficits in dry years. Consequently the impacts of droughts caused by large-scale weather patterns such as the PDO are of particular concern in boreal deciduous forests (Hogg et al., 2008). Soil water deficits also lower R_e, partially offsetting the effects of low precipitation on NEP (Barr et al., 2007; Ciais et al., 2005; Krishnan et al., 2006).

Although extensive observations have been published about the effects of weather on NEP, process-based hypotheses are needed to synthesize our understanding of these effects and to support predictions of ecosystem productivity under future changes in weather and climate. Such hypotheses may be formulated in process-based ecosystem models and tested with measurements of T_a and precipitation effects on forest net CO_2 exchange. In previous modelling work, earlier spring warming was shown to hasten the onset of net CO_2 uptake and thereby raise annual NEP of boreal coniferous and deciduous forests (Arain et al., 2002; Grant et al., 2008). Hotter summers were shown to lower net CO_2 uptake and hence annual NEP of boreal and temperate coniferous forests through hydraulic effects on stomatal conductance (Arain et al., 2002, 2006; Grant et al., 2001a,b, 2008). Lower summer precipitation was shown to hasten soil water deficits and thereby reduce net CO_2 uptake and annual NEP of boreal deciduous forests (Grant et al., 2006a).

This earlier work focussed on a limited number of sites over a few years (e.g. Arain et al., 2002; Grant et al., 2008), or on several sites over 1 year (e.g. Yuan et al., 2008). However if model hypotheses for weather effects are to be shown to be robust, then they must be tested with diverse data sets recorded at several sites differing in weather and productivity. The lengthening instrumental record of CO_2 exchange at EC flux towers along a transcontinental transect of forest stands in the Fluxnet-Canada Research Network (FCRN) now provides an opportunity to test model hypotheses for impacts of T_a and precipitation associated with large-scale weather patterns on regional forest CO_2 exchange. We therefore propose to build upon earlier modelling work by using these hypotheses to attribute interannual variability in NEP to changes in T_a and precipitation associated with large-scale weather events at all mature sites in the FCRN over the entire period of EC measurements to the end of 2006. Attribution will be made through the ecosystem model *ecosys* (Grant et al., 2008), corroborated by EC CO_2 and energy fluxes, wood growth increments from inventory studies, and from remotely-sensed vegetation indices recorded during this period.

2. Methods

The key algorithms governing the simulation of NEP in *ecosys* are described in Supplement to this article, in which equations and variables referenced in the text below are listed in Appendices A–C.

NEP from *ecosys* was compared with that from EC flux towers at hourly, daily and annual time scales over all mature forest stands in the FCRN from 1998 to 2006 (Fig. 1), gap-filled according to established FCRN protocol as described in Barr et al. (2004). Model performance was evaluated through regression analyses of modelled hourly CO_2 fluxes on measured hourly-averaged CO_2 fluxes in which both 1/2-hourly values were considered accurate. Based on random errors in EC flux measurements derived over forested sites by Richardson et al. (2006), agreement was considered acceptable when slopes and intercepts from these regressions were within 0.1 of one, and within 1 $\mu mol\ m^{-2}\ s^{-1}$ of zero, respectively. Agreement was also indicated by root mean squares for differences (RMSD) between measured and modelled

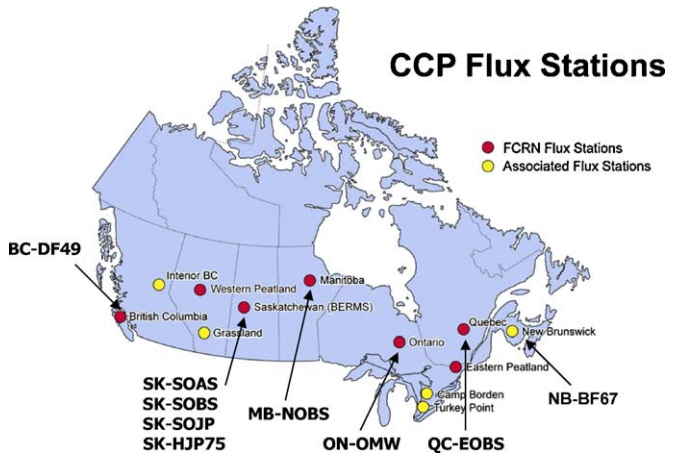

Fig. 1. Locations of flux stations in the Fluxnet-Canada Research Network. For descriptions of station sites, see Table 1.

fluxes not significantly greater ($P < 0.05$) than root mean squares for error (RMSE) in the measured fluxes derived over comparable forest stands by Richardson et al. (2006).

To examine the potential for remote-sensing products to support model results, seasonal changes in LAI from *ecosys* were compared with those in NDVI from MODIS data recorded over a 2.25 km × 2.25 km area around each FCRN site. MODIS NDVI was extracted from the national scale MODIS dataset produced in the J35 project of the ESS climate change program (ERCC).

Before these comparisons could be made, the model had to reproduce site conditions by simulating site histories. This was accomplished by initializing *ecosys* at each site with the biological properties of the key overstory and understory species, and with the physical and chemical properties of the dominant soil type at each FCRN site (Table 1). Each vegetation functional type (coniferous or deciduous, overstory or understory) had identical properties at each site in which it was present, except for those properties associated with timing of key phenological events (e.g. Grant et al., 2007a) which were adapted to the climate zone (temperate or boreal) at each site. Model parameters are derived from independent experiments and so remained unchanged from those used in earlier studies (e.g. Grant et al., 2007b, 2008). *Ecosys* was also initialized with stocks of coarse and fine residue estimated to remain after a stand-replacing fire. The model was then run from forest seeding to maturity under repeating sequences of continuous hourly weather data (radiation, T_a, dewpoint or RH, wind speed and precipitation) recorded during the period of measurement at each FCRN site (Table 1). The modelled forests were then burnt or logged, according to site disturbance history, reseeded and regrown under continuing sequences of weather data until they reached the current age of the forest stands at each site (Table 1). The model was run at all sites for *ca*. 200 years before comparison with measured data, so that model results were independent of initial conditions. A background mortality rate of 1.2% (QC-EOBS) or 0.8% (all other sites) per year was applied to forest stands during the model runs, simulating natural self-thinning (Aakala et al., 2007). These rates were applied monthly to populations with trees of uniform biomass, so that both biomass and population were reduced to the same extent by each mortality event. All biomass removed by mortality was added to surface or subsurface litter stocks in the model. During the last 150 years of the model runs, C_a rose exponentially from 280 μmol mol^{-1} to 385 μmol mol^{-1}, and precipitation NH_4^+ and NO_3^- concentrations used to simulate wet N deposition rose exponentially from historical values based on Holland et al. (1999) to current values based on Meteor-

Table 1
Key attributes of vegetation, soil and climate at FCRN sites.

Site	BC-DF49	SK-SOAS	SK-SOBS	SK-SOJP	SK-HJP75	MB-NOBS	ON-OMW	QC-EOBS	NB-BF67
Latitude N	49.9	53.6	54.0	53.9	53.9	55.9	48.2	49.7	46.4
Longitude W	125.3	106.2	105.1	104.7	104.6	98.5	82.2	74.3	67.1
Established	Fire 1943	Fire 1919	Fire 1879	Fire 1929	Logged 1975	Fire 1845	Logged 1937	Fire 1898	Logged 1967
Overstory	Douglas-fir	Aspen	Black spruce	Jack pine	Jack pine	Black spruce	Spruce, birch, aspen, balsam fir	Black spruce	Balsam fir
Understory	Sparse	Hazelnut	Feather moss	Lichen, green alder	Lichen, green alder	Feather, sphagnum moss	Shrubs, moss	Feather moss	
Soil type	Humo-ferric podzol	Orthic gray luvisol	Gleyed cumic humic regosols	Glacial till	Glacial till	Gleyed cumic humic regosols		Ferro-humic podzol	Humo-ferric podzol
LFH (cm)	0–6	8–10	20–30	5	5	10–160	15	10	7
Soil texture	Gravelly sandy loam	Sandy clay loam	Sandy clay	Sand	Sand	Coarse	Silty, very fine sand	Gravelly loamy sand	Sandy clay loam
MAT (°C)	8.3	0.4	0.4	0.4	0.4	−3.2	7.8	0.0	2.1
Precipitation (mm y^{-1})	1461	467	457	467	467	517	1010	961	1196
Period of measurement	1998–2006	1994–2006	1994–2006	2000–2006	2004–2006	1994–2006	2004–2006	2004–2006	2004–2005
Site references	Morgenstern et al. (2004); Jassal et al. (2007)	Barr et al. (2007); Krishnan et al. (2006)	Gaumont-Guay et al. (2008); Krishnan et al. (2008)	Kljun et al. (2007)	Howard et al. (2004)	Dunn et al. (2007)	McCaughey et al. (2006)	Bergeron et al. (2007)	Hassan et al. (2006)
Ecosys references	Grant et al. (2007b)	Grant et al. (2006a)	Grant et al. (2001b, 2008)	Grant et al. (2007a)	Grant et al. (2007a)	Grant et al. (2001a, 2008)		Grant et al. (2008)	

Table 2
Mean annual temperatures (MAT), annual precipitation, followed by intercepts (a), slopes (b), coefficients of determination (R^2), root mean square of differences (RMSD), and number of accepted eddy covariance (EC) fluxes from regressions of hourly modelled CO_2 fluxes *vs.* hourly-averaged EC CO_2 fluxes at all mature FCRN sites from 1998 to 2006.

Site	Year	MAT (°C)	Precipitation (mm)	a (μmol m^{-2} s^{-1})	b	R^2	RSMD (μmol m^{-2} s^{-1})	n
BC-DF49	1998	9.10	1844	0.2	1.10	0.75	3.3	5187
	1999	7.64	1913	0.4	1.09	0.77	3.1	4982
	2000	8.21	1127	0.4	1.02	0.76	3.5	4954
	2001	8.09	1166	0.4	1.01	0.77	3.3	4990
	2002	8.48	1222	0.5	1.07	0.75	3.4	5026
	2003	8.48	1621	0.3	1.04	0.77	3.4	5277
	2004	8.77	1404	0.6	0.99	0.75	3.8	4362
	2005	8.31	1467	0.9	0.96	0.77	3.8	4388
	2006	8.40	1809	0.1	1.02	0.76	3.4	5233
SK-SOAS	1998	3.31	547	0.3	1.14	0.82	2.6	5738
	1999	2.94	479	0.3	1.09	0.80	2.6	6644
	2000	1.31	484	0.1	1.09	0.83	2.5	6023
	2001	3.01	235	−0.1	1.05	0.79	2.9	5729
	2002	0.07	289	−0.1	1.16	0.82	2.1	5811
	2003	1.88	261	0.2	1.19	0.80	2.2	6062
	2004	0.83	741	0.1	1.26	0.87	1.9	6329
	2005	2.46	609	0.5	1.19	0.83	2.4	6457
	2006	3.04	636	0.1	1.12	0.85	2.7	5994
SK-SOBS	1999	2.65	435	0.2	1.02	0.73	1.9	3725
	2000	1.11	489	0.2	0.98	0.74	1.7	5244
	2001	2.84	264	0.4	1.08	0.75	1.7	5196
	2002	0.17	369	0.1	1.06	0.75	1.6	5171
	2003	1.07	313	0.3	1.17	0.75	1.6	5127
	2004	−0.10	779	0.2	0.95	0.74	1.7	4970
	2005	1.83	598	0.2	1.01	0.76	1.6	4987
	2006	2.40	646	0.4	1.04	0.72	1.8	4605
SK-SOJP	2000	0.96	379	0.3	1.01	0.65	1.7	5209
	2001	2.98	307	0.5	1.12	0.63	1.6	5295
	2002	0.74	429	0.3	1.12	0.63	1.5	5188
	2003	1.39	262	0.2	1.02	0.57	1.6	5380
	2004	−0.10	717	0.2	1.12	0.69	1.4	4762
	2005	1.68	584	0.2	1.07	0.66	1.5	5633
	2006	2.68	582	0.2	1.14	0.69	1.3	4801
SK-HJP75	2004	−0.16	538	0.5	1.07	0.72	1.6	3667
	2005	1.82	645	0.4	1.05	0.67	1.6	5379
	2006	2.41	612	0.4	1.12	0.67	1.5	4565
MB-NOBS	1998	−0.50	389	0.2	1.00	0.74	1.4	5871
	1999	−0.16	308	0.3	1.00	0.79	1.4	6345
	2000	−1.75	390	0.1	0.91	0.70	1.4	4861
	2001	−0.18	373	0.2	0.98	0.75	1.5	4993
	2002	−2.09	534	0.0	0.98	0.78	1.3	5444
	2003	−0.54	355	0.2	1.10	0.74	1.4	5412
	2004	−2.34	463	0.1	1.04	0.82	1.2	4876
	2005	0.32	773	0.3	1.08	0.78	1.3	5001
	2006	1.81	415	0.2	1.04	0.77	1.4	4282
ON-MWB	2004	1.97	924	0.0	0.98	0.66	3.0	4540
	2005	3.72	700	0.5	1.13	0.69	2.7	5413
	2006	4.18	790	0.5	1.09	0.72	2.7	6217
QC-EOBS	2004	−0.35	1027	0.0	0.97	0.74	1.7	5310
	2005	1.59	974	0.3	1.12	0.78	1.5	6531
	2006	2.25	867	0.1	1.10	0.77	1.5	6367
NB-BFR67	2004	3.10	714	0.2	1.12	0.74	3.0	3536
	2005	4.27	641	0.5	1.18	0.70	2.8	5232

ological Service of Canada (2004). Atmospheric concentration of NH_3 used to simulate dry N deposition was maintained at 0.0025 μmol mol^{-1}.

3. Results

3.1. Modelled vs. measured CO_2 fluxes under contrasting weather

The study period from 1998 to 2006 included three large-scale weather events: a combined ENSO/PDO event from 1998 to 1999/2000, a drought from 2001 to 2003, possibly exacerbated by a weak ENSO event in 2002/2003, and warming from 2004 to 2006. During the 1998–1999 ENSO/PDO event, higher mean annual temperatures (MAT) were recorded at all FCRN tower sites active during the El Niño phase in 1998, and lower MAT during the subsequent La Niña phase in 1999–2000 (Table 2). The 2001–2003 drought caused annual precipitation to decline by as much as 50% from long-term averages at some mid-continental sites in SK (Table 2). The drought was terminated by abnormally cool and rainy weather during 2004, followed by rises in MAT of 2–3 °C through 2005 and 2006 at all continental sites (Table 2).

Regressions of hourly modelled CO_2 fluxes *vs.* hourly-averaged measured CO_2 fluxes for all FCRN site-years to 2006 gave intercepts mostly within 0.5 μmol m^{-2} s^{-1} of zero, and slopes mostly

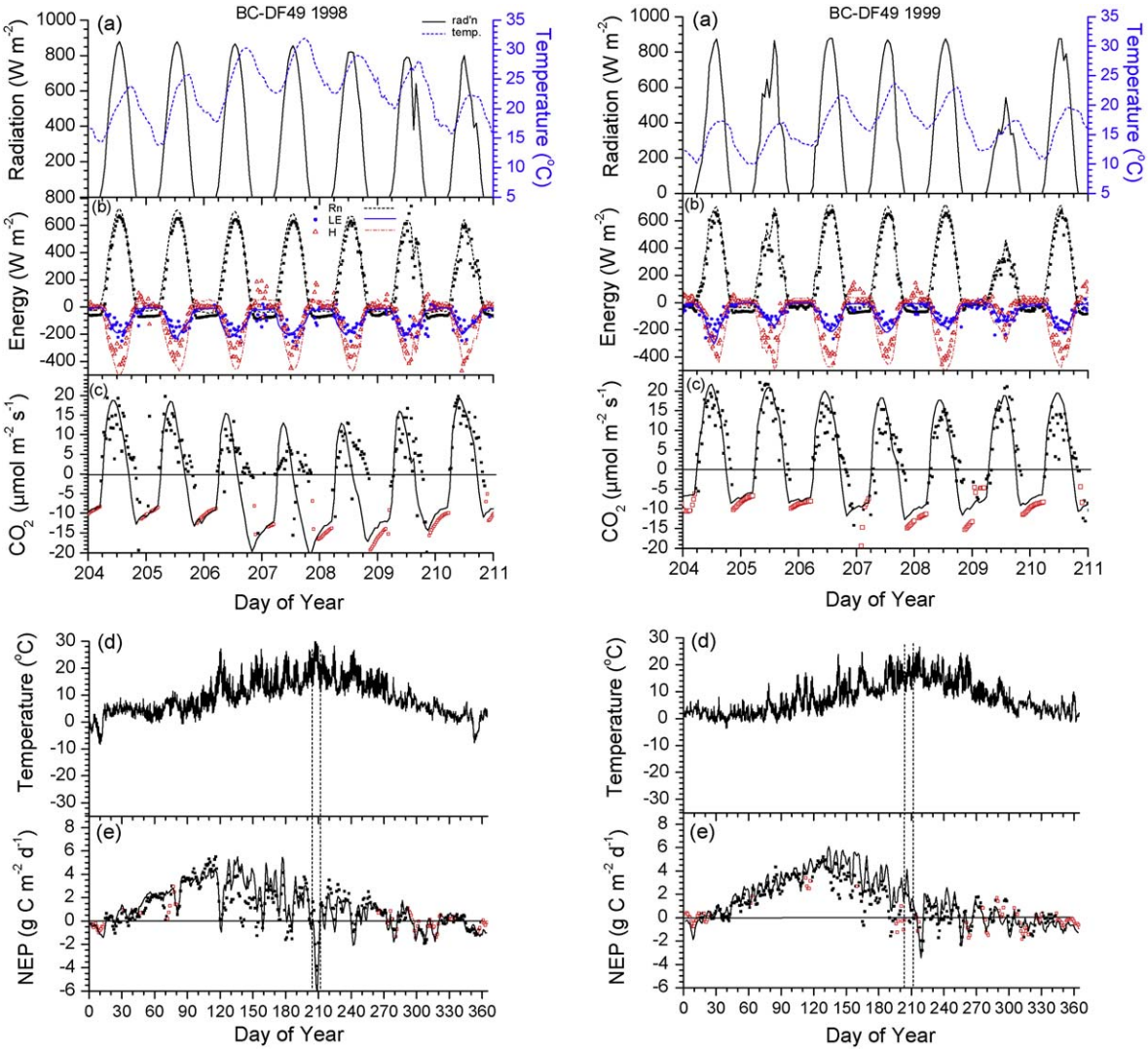

Fig. 2. (a) Solar radiation and air temperature, (b) net radiation, latent and sensible heat fluxes, (c) net CO_2 exchange measured or modelled (symbols or lines in b and c) during DOY 205–211 (24–30 July) in 1998 and 1999, and (d) air temperature and (e) daily net ecosystem productivity measured or modelled (symbols or lines in e) during the entire year in 1998 and 1999 over BC-DF49 (see Table 1). Positive or negative values denote downward or upward fluxes respectively. Open symbols in (c) represent gap-filled 1/2-hourly fluxes, those in (e) represent daily net fluxes consisting of >24 1/2-hourly gap-filled fluxes.

between 0.98 and 1.15 (Table 2). These regression parameters indicated minimal bias, but a tendency for variation in modelled fluxes slightly to exceed that in EC measurements, possibly because EC fluxes were not corrected for incomplete energy balance closure which was 85–90% for most site-years. Values for coefficients of determination (R^2) and root mean squares for differences (RMSD) between modelled and EC fluxes were 0.75–0.85 ($P < 0.0001$) and 2–4 μmol m^{-2} s^{-1} at more productive sites (BC-DF49 and SK-SOAS), and 0.65–0.75 and 1.2–1.8 μmol m^{-2} s^{-1} at less productive sites (e.g. other SK, MB and QC sites). These RMSDs were less than or comparable to those from earlier modelling studies at these sites (Amthor et al., 2001; Arain et al., 2002; Grant et al., 2005, 2006b; Yuan et al., 2008), indicating ongoing progress in modelling CO_2 exchange over temperate and boreal forests. Hourly RMSDs were also smaller than random errors in EC CO_2 flux measurements at forest sites, estimated by Richardson et al. (2006) to rise linearly from 1.4 μmol m^{-2} s^{-1} to 5.2 μmol m^{-2} s^{-1} for CO_2 influxes from 0 μmol m^{-2} s^{-1} to 20 μmol m^{-2} s^{-1} and from 0.6 μmol m^{-2} s^{-1} to 6.9 μmol m^{-2} s^{-1} for CO_2 effluxes from 0 μmol m^{-2} s^{-1} to 10 μmol m^{-2} s^{-1}, the range of fluxes measured at the FCRN sites. Much of the unexplained variance in EC fluxes could be attributed to a random error of *ca.* 20% in EC methodology (Wesely and Hart, 1985), mostly attributed in this study to three sources (Grant et al., 2008):

(1) Variable EC CO_2 influxes frequently recorded during daylight hours with apparently stable 1/2-hourly-averaged weather conditions, during which scatter in the EC CO_2 influxes caused modelled values to exceed most of the measured values (e.g. DOY 215 *vs.* 214 at SK-SOAS 2001 in Fig. 4c). This scatter in daytime EC fluxes requires further examination.
(2) Anomalously large CO_2 effluxes occasionally measured during the hour or two after sunrise (e.g. DOY 214, 215 at SK-SOJP 2001 in Fig. 5c) which were not modelled. These effluxes were usually associated with large changes in canopy CO_2 storage, likely caused by rapidly changing turbulence with early morning warming.
(3) Scatter in nighttime CO_2 effluxes measured by EC even under favourable wind conditions (e.g. DOY 207 and 209 at BC-DF49 1999 in Fig. 2c).

Parameters from regressions of modelled on EC fluxes did not vary significantly with MAT or annual precipitation at any of the sites (Table 2), indicating consistency of model performance over

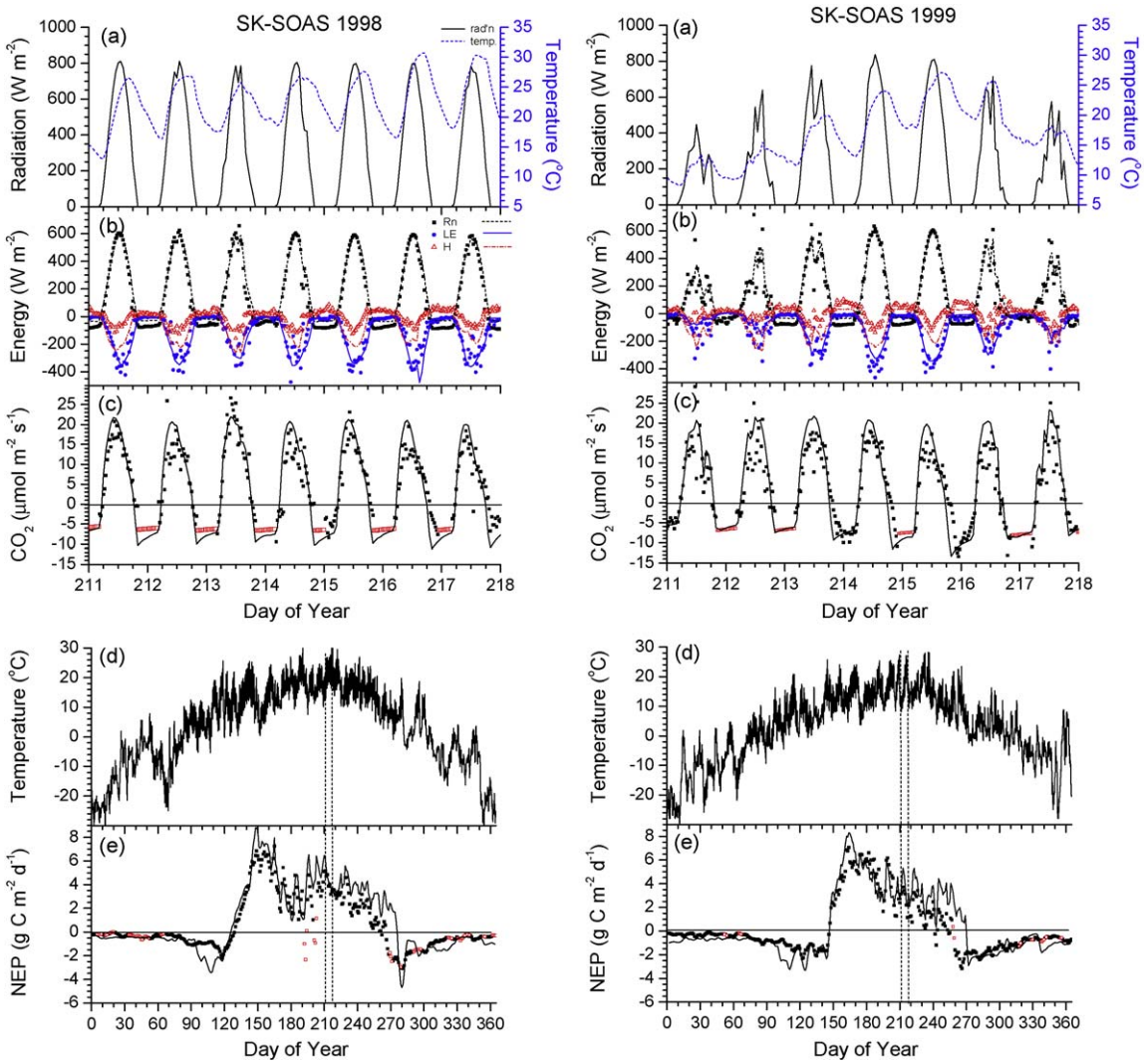

Fig. 3. (a) Solar radiation and air temperature, (b) net radiation, latent and sensible heat fluxes, (c) net CO_2 exchange measured or modelled (symbols or lines in b and c) during DOY 212–218 (31 July to 6 August) in 1998 and 1999, and (d) air temperature and (e) daily net ecosystem productivity measured or modelled (symbols or lines in e) during the entire year in 1998 and 1999 over SK-SOAS (see Table 1). Positive or negative values denote downward or upward fluxes respectively. Open symbols in (c) represent gap-filled 1/2-hourly fluxes, those in (e) represent daily net fluxes consisting of >24 1/2-hourly gap-filled fluxes.

the range of weather recorded at all sites during the FCRN study period. However there was a tendency ($P = 0.18$) for the regression slope b to rise with lower MAT at SK-SOAS, indicating slightly larger modelled *vs*. measured fluxes during cooler years at this site.

3.2. ENSO and CO_2 exchange 1998–1999

High temperature events during the 1998 El Niño (e.g. Fig. 2a) caused diurnal declines in CO_2 influxes, driven by GPP (Eq. [C1]) and rises in CO_2 effluxes, driven by R_a (Eq. [C12]) and R_h (Eq. [A11]), at BC-DF49 that did not occur under more moderate temperatures in 1999 (e.g. a high T_a event during the week of DOY 205–211 in Fig. 2c). Declines in CO_2 influxes under higher temperature (T_a) were modelled from hydraulic constraints to water uptake imposed by large axial resistivity of conifer roots and boles, particularly that of the tall boles (33 m) modelled at this site (Eqs. [B11 and B12]). These constraints forced declines in midafternoon canopy water potential (ψ_c) (Eq. [B13]) and hence stomatal conductance (g_c) (Eq. [B3]) under higher vapor pressure deficit (D) when equilibrating water uptake (Eqs. [B5 and B6]) with transpiration (Eq. [B1]) in the model (Grant et al., 2001a,b, 2007a,b, 2008). Declines in midafternoon g_c prevented modelled latent heat fluxes (LE) from rising with T_a and D, consistent with EC measurements (Fig. 2b). Rising T_a hastened autotrophic and heterotrophic respiration (R_a and R_h from Eqs. [C13] and [A13], respectively) in the model, raising CO_2 effluxes (Fig. 2e) and further reducing CO_2 influxes. These changes in CO_2 fluxes were neither modelled nor measured under lower T_a recorded in 1999 (Fig. 2c). Regressions of modelled on measured CO_2 fluxes during DOY 205–211 in 1998 and 1999 indicated a model bias towards greater effluxes under high *vs*. low T_a (more negative a in Table 3, although measured effluxes were few during these periods (Fig. 2c)). However there was no bias in model sensitivity to T_a (same b in Table 2) and RSMDs between modelled and measured fluxes were comparable to random errors in EC fluxes estimated by Richardson et al. (2006).

Declines in CO_2 influxes plus rises in CO_2 effluxes caused sharp reductions in daily NEP (=daily sums of CO_2 fluxes) modelled and measured during several warming events in 1998 (Fig. 2d and e), including that during DOY 205–211 (Fig. 2a–c). Such events were less frequent during 1999, allowing NEP modelled and measured during May, June and July at BC-DF49 to remain larger than that in 1998.

High temperature events during the 1998 El Niño at SK-SOAS (e.g. Fig. 3a) frequently followed those at BC-DF49 (e.g. high T_a during the week of DOY 212–218 in Fig. 3a) because weather

Table 3
Intercepts (a), slopes (b), coefficients of determination (R^2), root mean square of differences (RMSD), and number of accepted eddy covariance (EC) fluxes from regressions of hourly modelled CO_2 fluxes *vs*. hourly-averaged EC CO_2 fluxes during periods selected for temperature or water stress events at mature FCRN sites from 1998 to 2006.

Site	Year	DOY	Event	a (μmol m^{-2} s^{-1})	b	R^2	RSMD (μmol m^{-2} s^{-1})	n
BC-DF49	1998	205–211	High T_a	−3.6	1.12	0.52	5.2	109
	1999	205–211	Low T_a	−0.9	1.12	0.72	4.2	110
SK-SOAS	1998	212–218	High T_a	−0.9	1.21	0.81	3.5	121
	1999	212–218	Low T_a	0.4	1.21	0.86	3.3	135
SK-SOAS	2001	211–217	Avg θ	−0.7	1.14	0.79	4.2	123
	2003	211–217	Low θ	1.1	1.57	0.77	2.4	112
SK-SOJP	2001	211–217	Avg. θ	0.4	0.82	0.47	3.1	111
	2003	207–213	Low θ	1.1	0.82	0.51	2.5	122
SK-SOAS	2004	232–238	Low T_a	1.2	1.28	0.94	2.0	124
	2006	232–238	Avg. T_a	0	1.26	0.91	2.7	136
ON-OMW	2004	232–238	Low T_a	2.6	1.34	0.59	3.2	130
	2006	232–238	Avg. T_a	2.9	1.03	0.72	3.8	99
BC-DF49	2004	203–209	High T_a	−2.3	1.18	0.65	4.5	109
SK-SOAS	2004	203–209	High T_a	1.0	1.18	0.87	3.6	131
NB-BF67	2004	207–213	High T_a	−0.4	1.01	0.83	3.2	1006

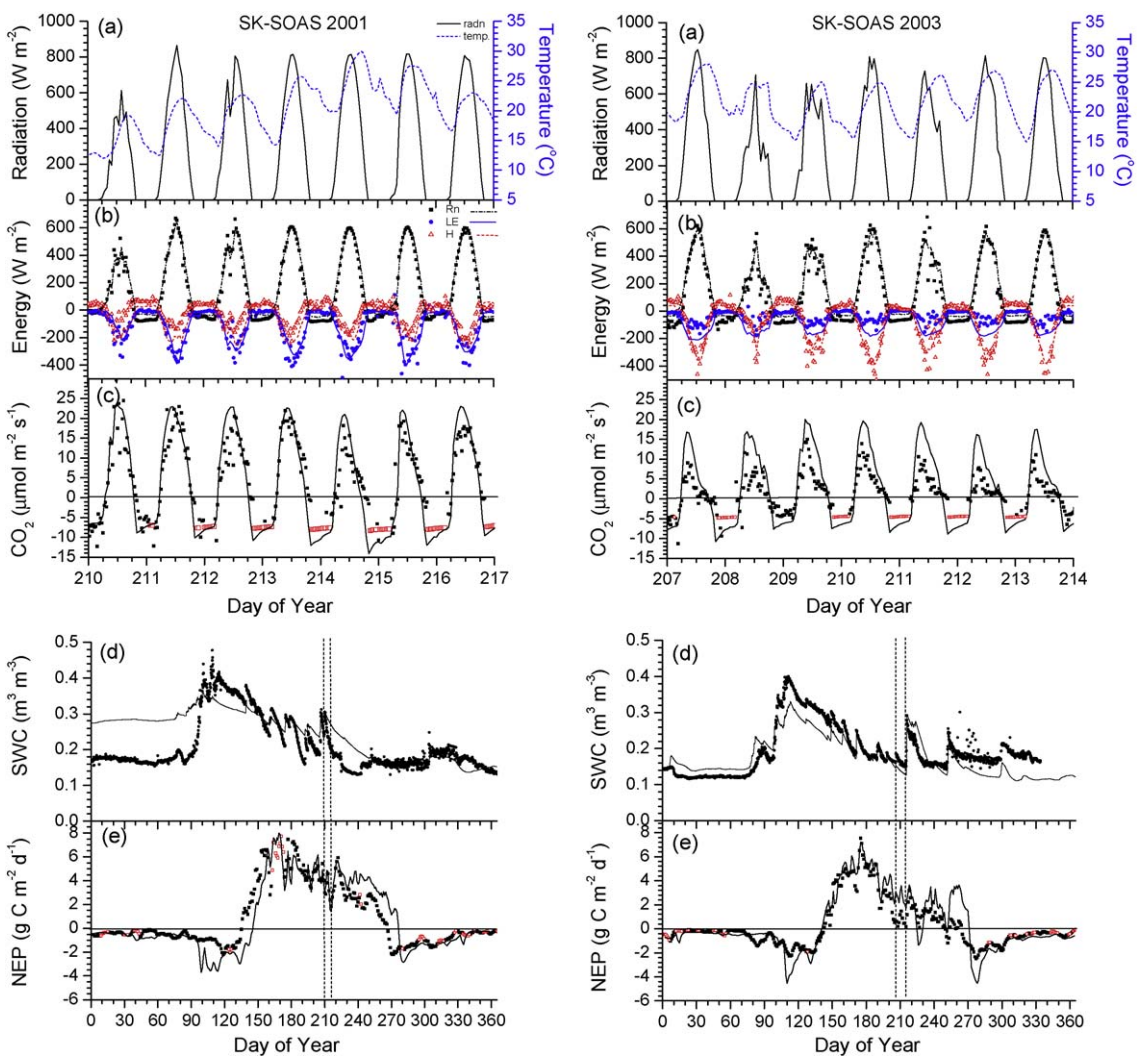

Fig. 4. (a) Solar radiation and air temperature, (b) net radiation, latent and sensible heat fluxes, (c) net CO_2 exchange measured or modelled (symbols or lines in b and c) during DOY 211–217 (30 July to 5 August) 2001 and DOY 208–214 (27 July to 2 August) 2003, and (d) soil water content 0–15 cm and (e) daily net ecosystem productivity measured (symbols) or modelled (lines) during the entire year in 2001 and 2003 over SK-SOAS (see Table 1). Positive or negative values denote downward or upward fluxes respectively. Open symbols in (c) represent gap-filled 1/2-hourly fluxes, those in (e) represent daily net fluxes consisting of >24 1/2-hourly gap-filled fluxes.

patterns in western North America tend to move from west to east. However at SK-SOAS these events did not reduce CO_2 influxes with respect to those under cooler weather in 1999, although very slight midafternoon declines were apparent under higher T_a in both years (Fig. 3c). In the model, lower axial resistivity of deciduous *vs.* coniferous roots and boles (Eqs. [B11 and B12]) reduced hydraulic constraints to water uptake, and hence midafternoon declines in ψ_c (Eq. [B13]) and g_c (Eq. [B3]) under higher D. These reduced constraints were indicated by rises in LE *vs.* H modelled and measured at SK-SOAS with rises in T_a and hence D (Fig. 3b). Consequently CO_2 influxes of aspen were less sensitive to higher T_a than were those of Douglas-fir (Fig. 3c *vs.* Fig. 2c). Meanwhile CO_2 effluxes driven by R_h in the model were comparatively more rapid in 1999 than in 1998 (e.g. DOY 216 in Fig. 3c), in spite of lower soil temperatures, because soil litter stocks in 1999 had grown with more rapid litterfall from greater NPP modelled under warmer weather in 1997 and 1998. Regressions of modelled on measured CO_2 fluxes during DOY 212–218 in 1998 and 1999 had similar parameters and statistics (Table 3), indicating no model bias in simulating high T_a effects on net CO_2 exchange at SK-SOAS. Comparison of EC CO_2 effluxes during this period was limited by inadequate nighttime turbulence in 1998.

Earlier and more sustained warming during the growing season of 1998 *vs.* 1999 at SK-SOAS (Fig. 3d) caused net C uptake modelled and measured in 1998 to begin *ca.* 3 weeks earlier in spring and to decline more slowly in late summer than it did in 1999 (Fig. 3e). However no such gain in net C uptake was apparent at BC-DF49 (Fig. 2e). Consequently the El Niño/La Niña phases of the 1998/1999 ENSO had contrasting effects on NEP at SK-SOAS and BC-DF49 (Fig. 3e *vs.* Fig. 2e).

3.3. Drought and CO_2 exchange 2001–2003

Although precipitation recorded at mid-continental sites declined sharply in 2001 (Table 2), soil water remaining after several years of above-average rainfall before 2001 allowed water stress to be largely avoided during the first year of the 2001–2003 drought. This soil water allowed rapid LE effluxes and CO_2 influxes to be maintained at SK-SOAS under rising T_a during mid-summer with only small declines in midafternoon values (e.g. during the week of DOY 211–217 in Fig. 4a–c). However soil drying in the third drought year of 2003 (Fig. 4d) caused lower soil water potential (ψ_s) and higher soil and root hydraulic resistances in the model (Eq. [B9]) that forced root water uptake (Eq. [B6]) to

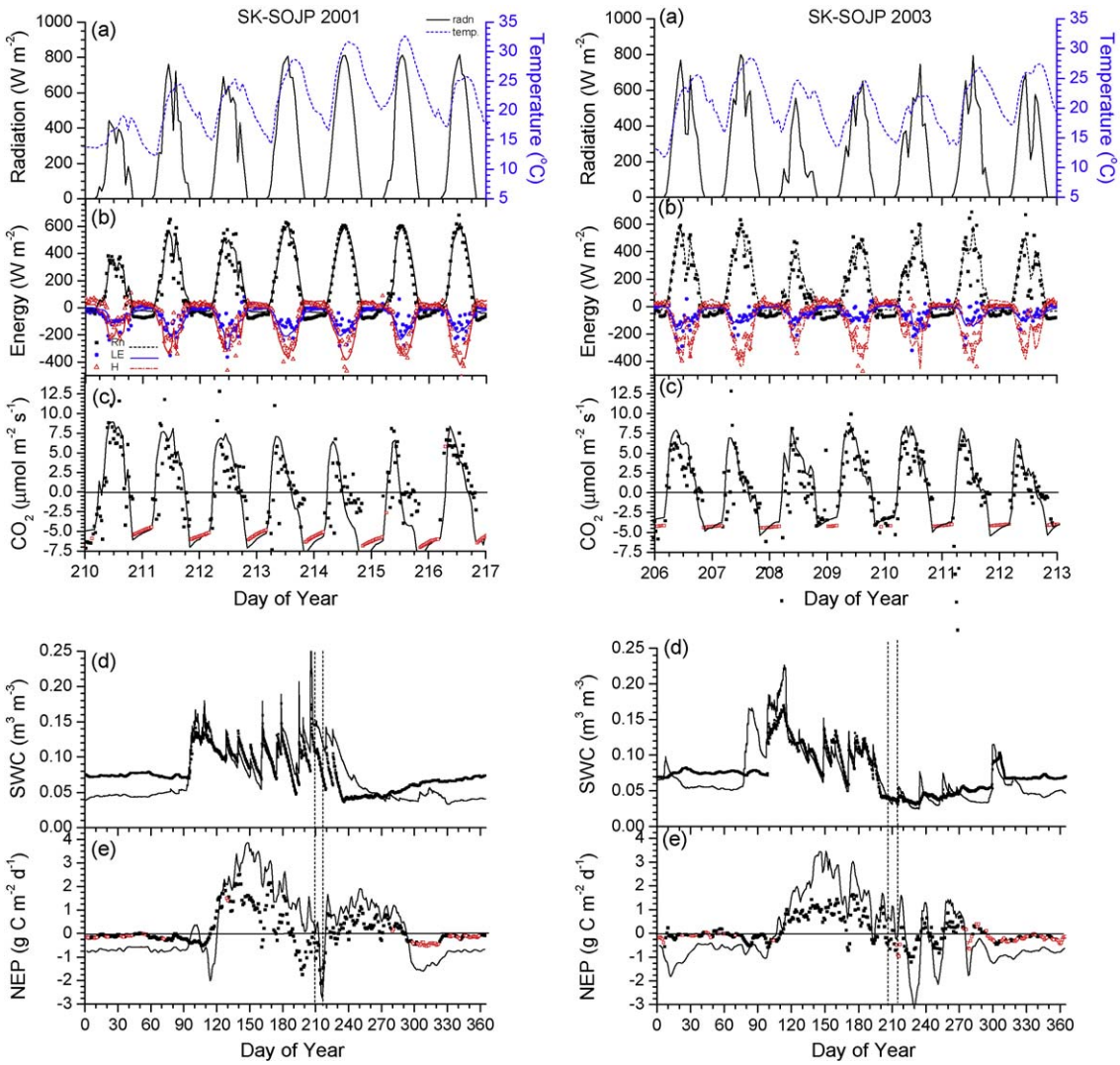

Fig. 5. (a) Solar radiation and air temperature, (b) net radiation, latent and sensible heat fluxes, (c) net CO_2 exchange measured or modelled (symbols or lines in b and c) during DOY 211–217 (30 July to 5 August) 2001 and DOY 207–213 (26 July to 1 August) 2003, and (d) soil water content 0–15 cm and (e) daily net ecosystem productivity measured (symbols) or modelled (lines) during the entire year in 2001 and 2003 over SK-SOJP (see Table 1). Positive or negative values denote downward or upward fluxes respectively. Open symbols in (c) represent gap-filled 1/2-hourly fluxes, those in (e) represent daily net fluxes consisting of >24 1/2-hourly gap-filled fluxes.

equilibrate with transpiration at lower ψ_c (Eq. [B13]) and hence g_c (Eq. [B3]) (Grant et al., 2006a). Lower g_c caused sharp declines in mid-summer LE effluxes (Eq. [B1]), and commensurate rises in H effluxes, to be modelled and measured during the same week in 2003 *vs*. 2001 (Fig. 4b and c). Lower g_c, combined with non-stomatal effects of lower ψ_c (Grant and Flanagan, 2007), also caused sharp declines in mid-afternoon CO_2 influxes to be modelled in 2003 (Eqs. [C4], [C6], [C7], [C9]). Slower CO_2 fixation drove slower R_a (Eq. [C16]), and drier soil drove slower R_h (Eqs. [A3 and A4]), reducing CO_2 effluxes in 2003 *vs*. 2001 (Fig. 4c). The net effects of soil drying on CO_2 exchange were apparent in the sharp declines of daily NEP modelled and measured after June 2003 (Fig. 4e). Regressions of modelled on measured CO_2 fluxes during DOY 211–217 in 2001 and 2003 indicated a bias to larger modelled CO_2 influxes during water stress at SK-SOAS ($b > 1$ during 2003 in Table 3).

Soil drying had a comparatively smaller effect on NEP at SK-SOJP (e.g. during the week of DOY 211–217 in 2003 *vs*. 2001 in Fig. 5) than at SK-SOAS (Fig. 4). Larger axial resistivity modelled in coniferous *vs*. deciduous trees (Eqs. [B11 and B12]), combined with low soil water holding capacity at SK-SOJP (Table 1), forced ψ_c and hence g_c (Eqs. [B13], [B3]) to decline during mid-summer warming at SK-SOJP in 2001 (Fig. 5a). These declines limited rises in LE effluxes (Eq. [B1]) under higher D (Fig. 5b), and forced mid-afternoon declines in CO_2 influxes (Eqs. [C4], [C6], [C7], [C9]) under higher T_a (Fig. 5c). These declines were similar to those during warming at BC-DF49 in 1998 (Fig. 2c), but were comparatively greater than those during the same warming event at nearby SK-SOAS (Fig. 4c). Such sharp declines in CO_2 influxes under higher T_a have also been observed in EC data recorded over pine stands elsewhere (Luyssaert et al., 2007). In the model, declines in g_c (Eq. [C4]), combined with non-stomatal effects of lower ψ_c (Eq. [C9]), forced lower intercellular CO_2 concentrations C_i during CO_2 uptake on drier soil under higher T_a (Grant and Flanagan, 2007). Such declines were consistent with lower C_i inferred from $\delta^{13}C$ measurements under higher potential evapotranspiration in boreal jack pine by Brooks et al. (1998).

Earlier soil drying at SK-SOJP in 2003 (Fig. 5d) forced further declines in modelled ψ_c and g_c, evident in lower mid-summer LE effluxes and relatively larger H effluxes (Fig. 5b). However consequent reductions in CO_2 influxes were largely offset by reductions in CO_2 effluxes from drier soil so that net CO_2 exchange in 2003 was similar to that over wetter soil in 2001 (Fig. 5c). Regressions of modelled on measured CO_2 fluxes during

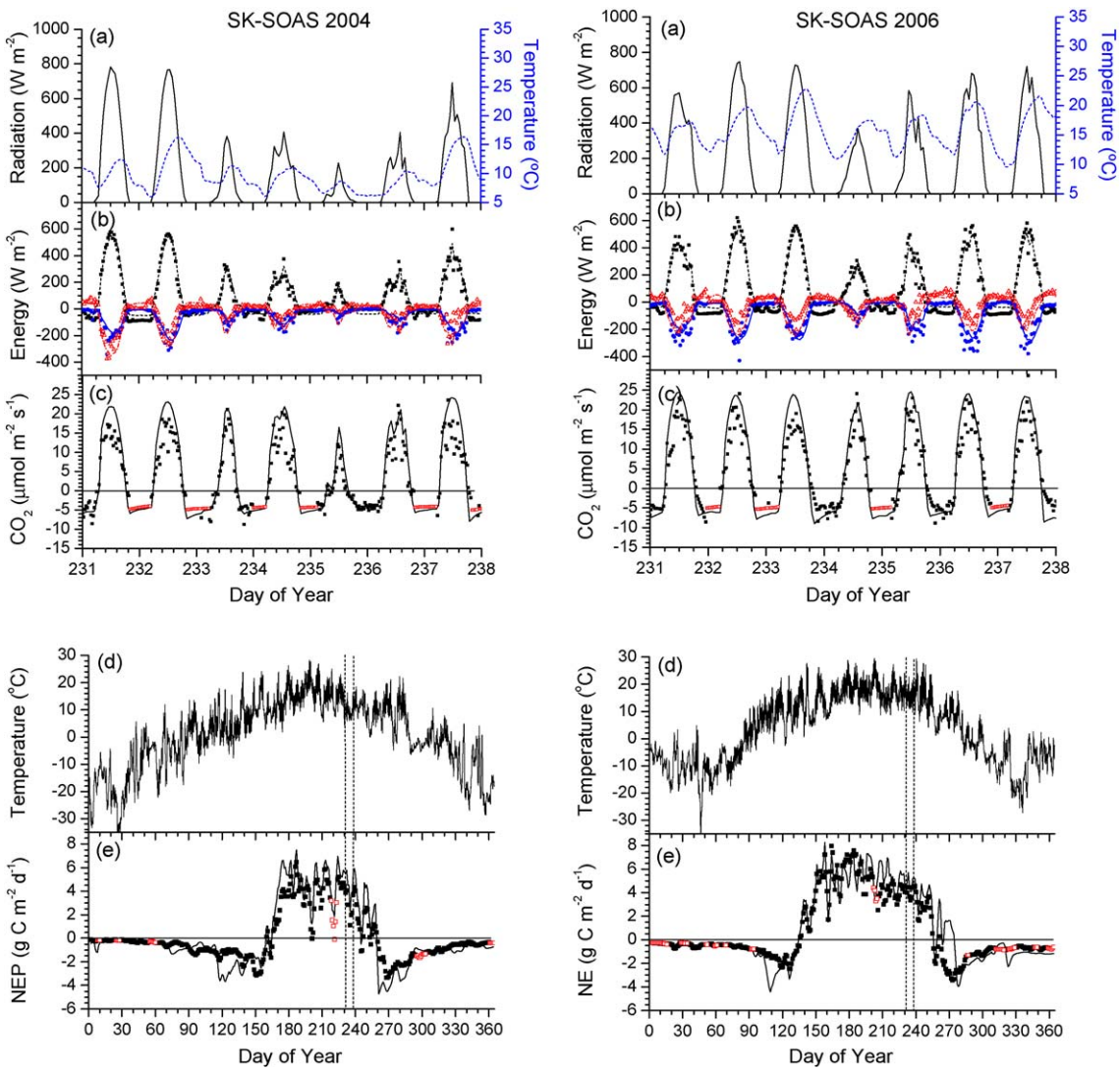

Fig. 6. (a) Solar radiation and air temperature, (b) net radiation, latent and sensible heat fluxes, (c) net CO_2 exchange measured or modelled (symbols or lines in b and c) during DOY 232–238 (20–26 August) 2004 and 2006, and (d) air temperature and (e) daily net ecosystem productivity measured or modelled (symbols or lines in e) during the entire year in 2004 and 2006 over SK-SOAS (see Table 1). Positive or negative values denote downward or upward fluxes respectively. Open symbols in (c) represent gap-filled 1/2-hourly fluxes, those in (e) represent daily net fluxes consisting of >24 1/2-hourly gap-filled fluxes.

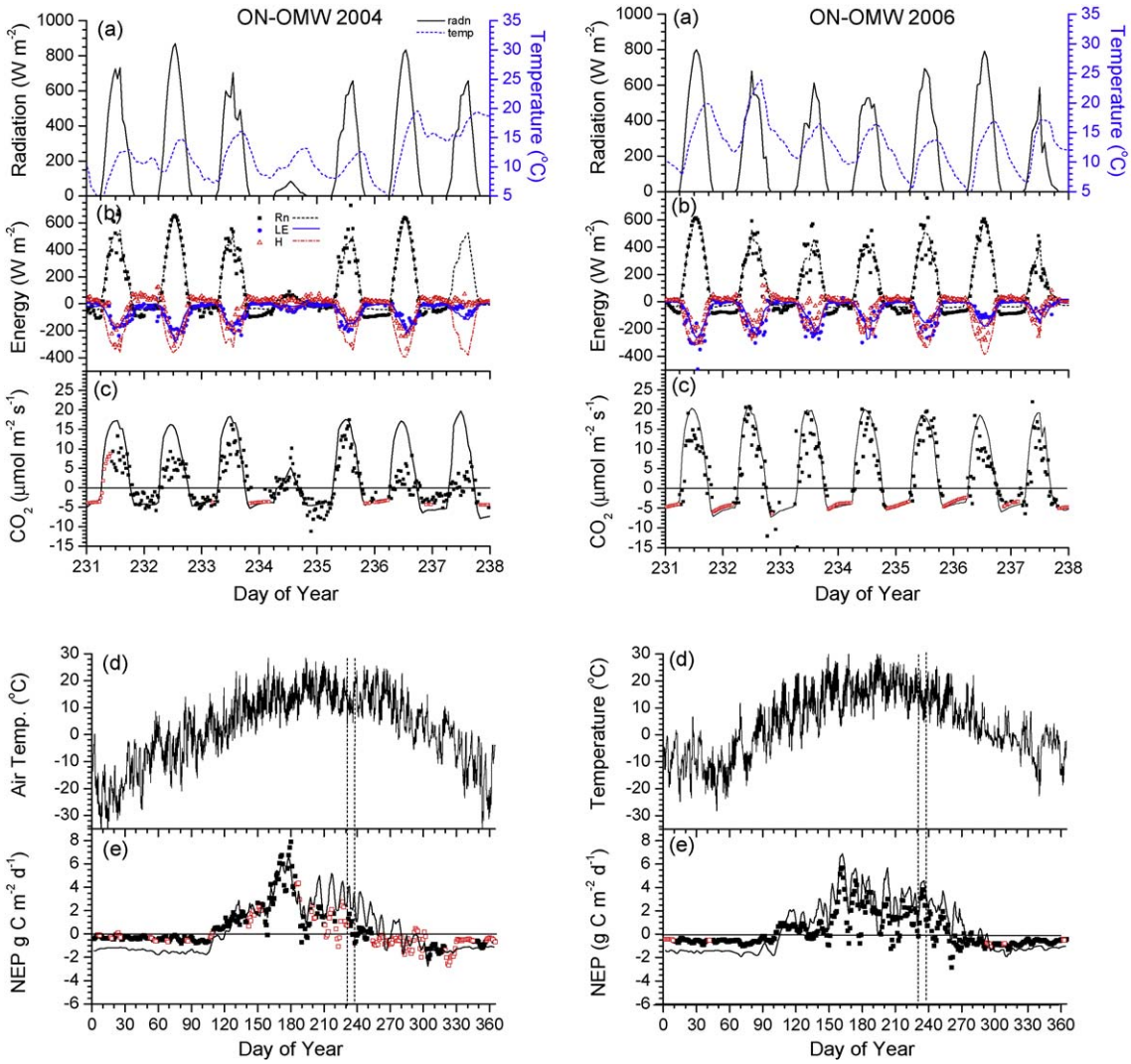

Fig. 7. (a) Solar radiation and air temperature, (b) net radiation, latent and sensible heat fluxes, (c) net CO_2 exchange measured or modelled (symbols or lines in b and c) during DOY 232–238 (20–26 August) 2004 and 2006, and (d) air temperature and (e) daily net ecosystem productivity measured or modelled (symbols or lines in e) during the entire year in 2004 and 2006 over ON-OMW (see Table 1). Positive or negative values denote downward or upward fluxes respectively. Open symbols in (c) represent gap-filled 1/2-hourly fluxes, those in (e) represent daily net fluxes consisting of >24 1/2-hourly gap-filled fluxes.

DOY 211–217 in 2001 and 2003 had similar parameters and statistics (Table 3), indication lack of model bias in simulating soil drying effects on CO_2 exchange at SK-SOJP. The effect of drought on annual NEP at SK-SOJP in 2003 (Fig. 5e) was therefore smaller than that at SK-SOAS (Fig. 4e), in spite of similar precipitation (Table 2). This smaller effect occurred because CO_2 influxes were more sensitive to higher T_a, and because evapotranspiration rates and hence soil drying were less rapid, in coniferous *vs*. deciduous forests (e.g. Figs. 2b, c and 5b, c *vs*. Figs. 3b, c and 4b, c). This smaller effect of drought on NEP at SK-SOJP than at SK-SOAS was also inferred from EC measurements by Kljun et al. (2007).

3.4. Warming and CO_2 exchange 2004–2006

Earlier warming at SK-SOAS in 2006 *vs*. 2004 caused earlier and more rapid net C uptake during spring (Fig. 6d and e), as was shown for this site in 1998 *vs*. 1999 (Fig. 3). In *ecosys*, timing of deciduous leafout and leafoff and of coniferous dehardening in spring and hardening in autumn was controlled by temporally integrated temperature above or below set thresholds under lengthening or shortening photoperiods, respectively. This timing gave reliable estimates of C uptake duration in cooler *vs*. warmer years, as found in earlier studies (Grant et al., 2008). Continued warming enabled more rapid net C uptake and energy exchange to be sustained by higher T_a and radiation in late summer 2006 (Eqs. [C6 and C7] from Eq. [C10]), while periods of cool, cloudy weather reduced net C uptake and energy exchange in 2004 (e.g. during the week of DOY 232–238 in Fig. 6a–c). Warm, clear weather allowed SK-SOAS to remain a continuous C sink until mid-September 2006, but cool, cloudy weather caused it to be a smaller and more variable sink during much of 2004 (Fig. 6e). Similar parameters and statistics from regressions of modelled on measured CO_2 fluxes during DOY 232–238 in 2004 and 2006 (Table 3) indicated a lack of model bias in simulating low T_a effects on CO_2 exchange at SK-SOAS.

The effects of earlier warming on spring net C uptake in 2006 *vs*. 2004 were less apparent at ON-OMW (Fig. 7d and e) than at SK-SOAS (Fig. 6d and e). However net C uptake and energy exchange at ON-OMW was maintained by comparatively warmer, sunnier weather during late summer 2006, while declining under cooler, cloudier weather in late summer 2004 (e.g. during the same week of DOY 232–238 in Fig. 7a–c), as at SK-SOAS (Fig. 6). Regressions of modelled on measured CO_2 fluxes during DOY 232–238 in 2004 and 2006 indicated a model bias towards larger CO_2 influxes under

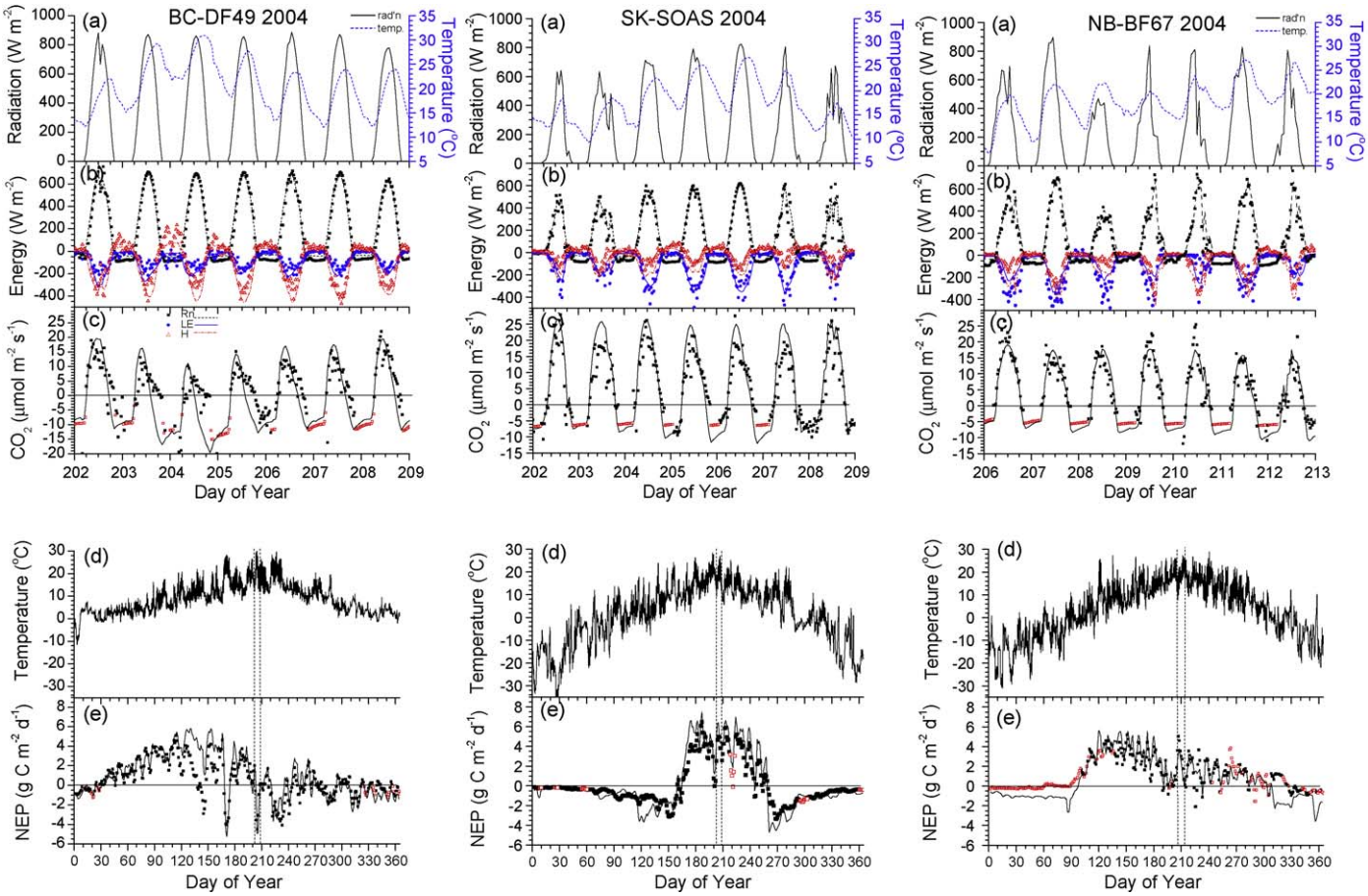

Fig. 8. (a) Solar radiation and air temperature, (b) net radiation, latent and sensible heat fluxes, (c) net CO_2 exchange measured or modelled (symbols or lines in b and c) during a warming event that passed through BC-DF49, SK-SOAS and NB-BF67 during DOY 203–213 (21–31 July) 2004, and (d) air temperature and (e) daily net ecosystem productivity measured or modelled (symbols or lines in e) during the entire year in 2004 at BC-DF49, SK-SOAS and NB-BF67 (see Table 1). Positive or negative values denote downward or upward fluxes respectively. Open symbols in (c) represent gap-filled 1/2-hourly fluxes, those in (e) represent daily net fluxes consisting of >24 1/2-hourly gap-filled fluxes.

cooler weather at ON-OMW ($b > 1$ during 2004 in Table 3). At both ON-OMW and SK-SOJP, warmer, clearer weather allowed sink activity to be sustained until mid-September 2006, but cooler, cloudier weather caused it to decline during August 2004 (Figs. 6e and 7e).

The spatial coherence of forest response to weather was examined during a warming event that passed successively over BC-DF49 (DOY 203–205), SK-SOAS (DOY 205–207) and NB-BF67 (DOY 211–213) during late July 2004 (Fig. 8a). This event did not raise LE, and lowered net CO_2 exchange, at BC-DF49 and NB-BF67, but raised LE and did not lower net CO_2 exchange at SK-SOAS (Fig. 8b and c), further demonstrating contrasting responses of coniferous and deciduous forests to comparable warming. The summer of 2004 was one of the warmest on record in the parts of North America most affected by Pacific weather patterns (Fig. 8d), with particularly adverse effects on NEP at BC-DF49 compared to other sites (Fig. 8e). Similar parameters and statistics from regressions of modelled on measured CO_2 fluxes during the warming events at BC-DF49, SK-SOAS and NB-BF67 (Table 3) indicated that the contrasting effects of warming events on CO_2 exchange at these sites was modelled consistently.

3.5. Weather and interannual variability in NEP 1998–2006

The transition from the warmer El Niño year in 1998 to the cooler La Niña year in 1999 caused annual NEP modelled and measured at BC-DF49 to rise (Fig. 9). Rises in summer temperatures and declines in precipitation from 2000 to 2004 (Table 2), including the weak El Niño event in 2003, caused declines in annual NEP to be modelled and measured at BC-DF49 after 1999. Several protracted warming events during summer 2004 had a particularly adverse effect on NEP (Fig. 8e), causing the lowest annual value modelled or measured at BC-DF49 from 1998 to 2006 (Fig. 9). Rises in precipitation from 2005 to 2006 enabled annual NEP to recover (Fig. 9).

NEP modelled at this site exceeded EC values by $\sim$100 g C m^{-2} y^{-1} although hourly-averaged CO_2 fluxes (Table 2) and phytomass growth (Fig. 12) agreed closely with measured values. Some of this discrepancy may be explained by large fluxes of DIC and DOC (30–70 g C m^{-2} y^{-1} and 1–3 g C m^{-2} y^{-1}, respectively, depending on rainfall) discharged in the model from this temperate, productive, high-rainfall site (Table 2), and assumed to degas elsewhere. This discharge was smaller than one of 100 ± 30 g C m^{-2} y^{-1} DIC estimated by Richey et al. (2002) from terrestrial sources in Amazon rainforests, and larger than one of 10–20 g C m^{-2} y^{-1} DIC + DOC estimated by Kling et al. (1991) from terrestrial sources in arctic tundra. In both ecosystems, these discharges were comparable to estimated rates of net C accumulation. There is evidence from recent studies of surface water chemistry at BC-DF49 that much of the DIC discharged at this site degasses locally, perhaps within the tower fetch area and so would be included in the EC measurements. However the rate of this degassing is currently unknown. Discharges of DIC and DOC modelled at other sites in this study were much smaller than those at BC-DF49 because these sites

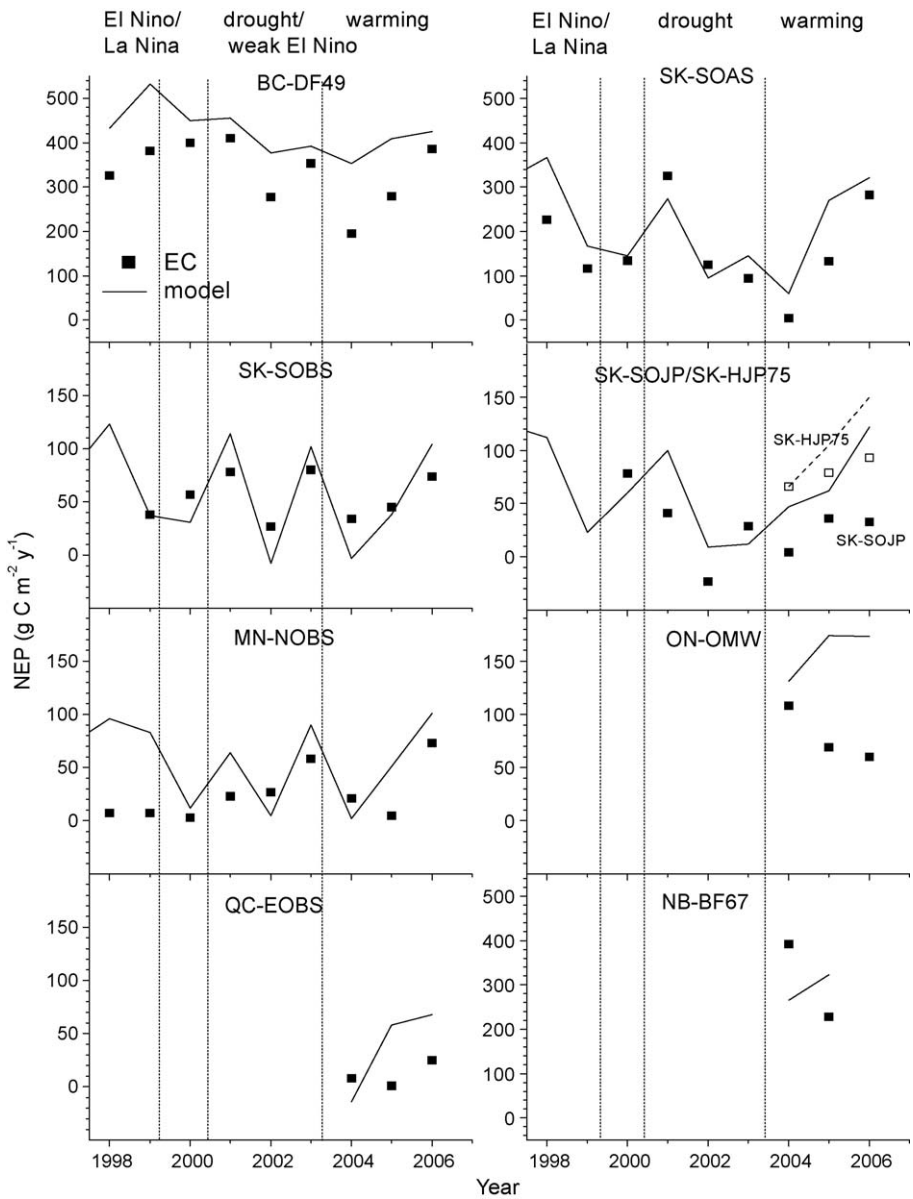

Fig. 9. Annual net ecosystem productivity modelled (lines) or derived from eddy covariance measurements according to FCRN gap-filling protocols (symbols) from 1998 to 2006 at all FCRN flux tower sites with mature stands (see Table 1).

were cooler, less productive and received less rainfall. Modelled NEP was closer to EC values at these sites (Fig. 9). Nonetheless DIC and DOC discharges may account for an important part of NEP, and need to be considered further in future studies of ecosystem productivity.

The 1998/1999 El Niño/La Niña transition caused a decline in NEP at SK-SOAS (Fig. 9), in contrast to the rise at BC-DF49, because warming/cooling affected net CO_2 exchange differently at these sites (Figs. 2, 3 and 8). Lower NEP modelled at SK-SOAS in 1999 was also partly attributed to more rapid R_h of litter (Fig. 3c) accumulated from greater litterfall during the more productive years 1997 and 1998 when higher T_a raised NPP. This carry-over of litter stocks in the model also caused declines in NEP at other sites following periods with higher NEP (e.g. 1999/2000 in Fig. 9). The only other flux tower active during the 1998/1999 ENSO was further north and east at MB-NOBS, where T_a was lower (Table 2) and ENSO effects on NEP were less apparent.

The drought from 2001 to 2003 lowered NEP in 2002 at all sites in SK (Fig. 9), in combination with low T_a (Table 2). The drought also lowered NEP in 2003 at SK-SOAS and to a lesser extent at SK-SOJP (Fig. 9) due to the effects of continued soil drying on water status of upland forest stands (Figs. 4 and 5). The rise in NEP modelled at SK-SOJP in 1998 and 2001, and the decline in 2002 and 2003 (Fig. 9), were consistent with the positive correlation of boreal jack pine growth with spring temperature and precipitation found by Brooks et al. (1998), and with March and June precipitation found by Savva et al. (2008). The drought did not reduce NEP in 2003 at the OBS sites in SK and MB where water uptake was sustained by water tables in poorly drained spruce stands (Fig. 9), as found experimentally by Kljun et al. (2007). Also precipitation recorded at these sites in 2003 was larger than that at the other SK sites (Table 2). Instead NEP at the OBS sites rose in 2003 with higher T_a (Table 2). NEP at MB-NOBS was also sustained by comparatively high precipitation in 2002. Smaller declines in NEP of coniferous *vs.* deciduous forests during drought have also been reported from EC measurements in Alaska by Welp et al. (2007), likely due to lower evapotranspiration rates (e.g. Fig. 5b *vs.* Fig. 4b).

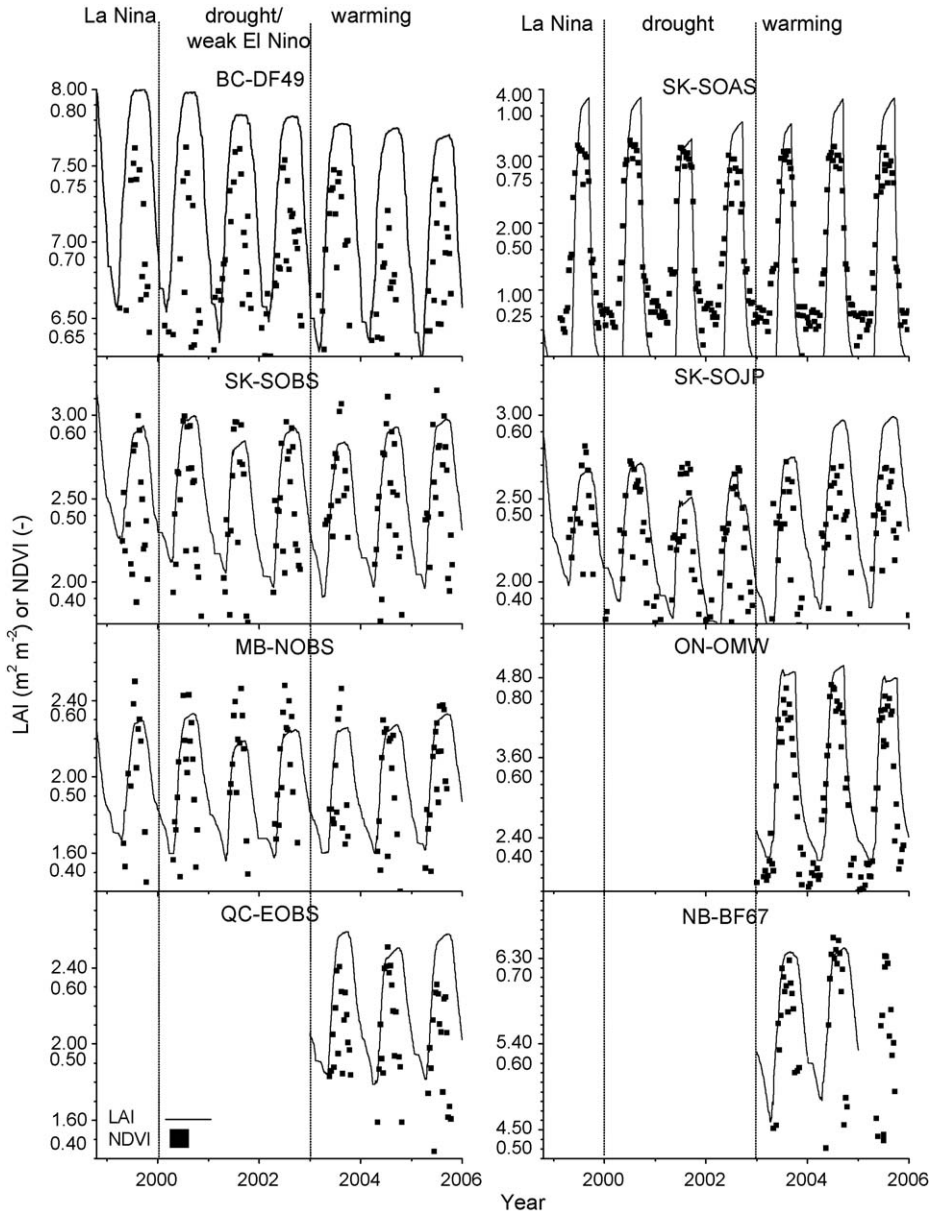

Fig. 10. Leaf Area Index modelled at (lines), or MODIS NDVI recorded over a 2.25 km × 2.25 km area centered around (symbols), all FCRN flux tower sites with mature stands from 1999 to 2006 (see Table 1).

Warming from 2004 to 2006 raised NEP at all sites in SK (e.g. Fig. 6) and MB, but experimental evidence for rises further east at ON-OMW, QC-EOBS and NB-BF67 was uncertain (Fig. 9). Rises in NEP modelled in 2005 were enhanced by lower R_h from smaller litter stocks that had declined with low NPP and hence litterfall during the less productive years from 2002 to 2004.

Modelled *vs*. EC-derived weather effects on NEP from 1998 to 2006 (Fig. 9) were to some extent reflected in comparisons of modelled LAI *vs*. MODIS NDVI recorded over the FCRN sites (Fig. 10). Both modelled LAI and recorded NDVI at BC-DF49 (Fig. 10) declined with NEP (Fig. 9) after 2001. Weather effects were not clearly apparent in peak values of modelled LAI or recorded NDVI at SK-SOAS, although the seasonal profiles of both were narrower in the cooler year 2004 than in the warmer year 2006 (Fig. 10), consistent with a shorter growing season (Fig. 6e) and lower NEP (Fig. 9). The drought lowered modelled LAI in 2002 and 2003 from those in 2001 at sites in SK and MB (Fig. 10), consistent with lower modelled and measured NEP (Fig. 9), but lowered NDVI only at SK-SOJP. Warming raised modelled LAI from 2004 to 2006 at all sites in SK and MB (Fig. 10), consistent with rises in NEP (Fig. 9), but raised NDVI only at SK-SOBS. Warming from 2004 to 2006 had no clear effects on LAI or NDVI at sites in ON, QC and NB. Comparison of modelled LAI with NDVI was limited by scatter in the MODIS data at the coniferous sites, but less so at the deciduous site (SK-SOAS) or the mixed wood site (ON-OMW).

3.6. Weather and interannual variability in wood growth

Interannual variability in modelled NEP (Fig. 9) caused interannual variability in changes of modelled C stocks, including wood growth (Fig. 11). Variability in wood C growth modelled at SK-SOAS and SK-SOJP followed a similar time course to that in wood C growth measured from tree ring chronologies by Hogg et al. (2008) and from dendrochronological stand reconstruction by Metsaranta and Lieffers (2009) respectively at a range of aspen and jack pine sites in the SK-SOAS and SK-SOJP ecozones (Fig. 11). Variability in the model included more rapid and then slower growth during the El Niño/La Niña phases of the 1998/1999 ENSO,

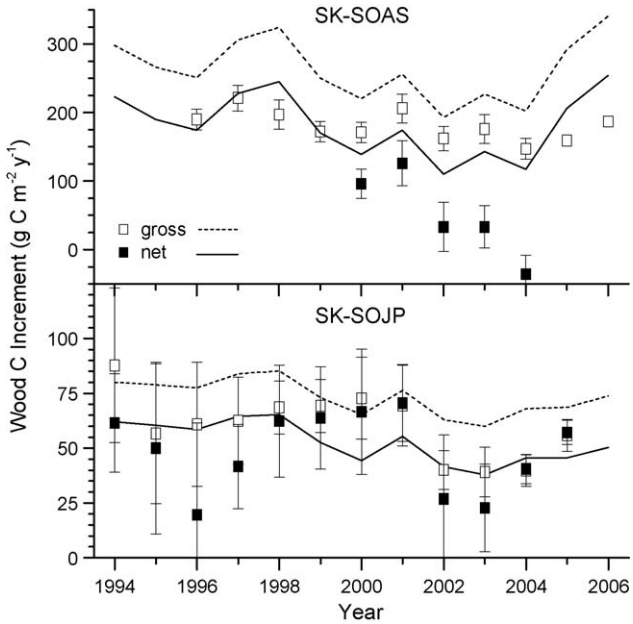

Fig. 11. Gross (excluding mortality) and net (including mortality) wood growth of aspen modelled at SK-SOAS (lines) and measured by Hogg et al. (2008) in 25 study areas across western Canada from 1996 to 2008 (symbols), and jack pine modelled at SK-SOJP (lines) and measured by Metsaranta and Lieffers, 2009 (symbols) from inventory plots in the boreal plains ecozone near SK-SOJP.

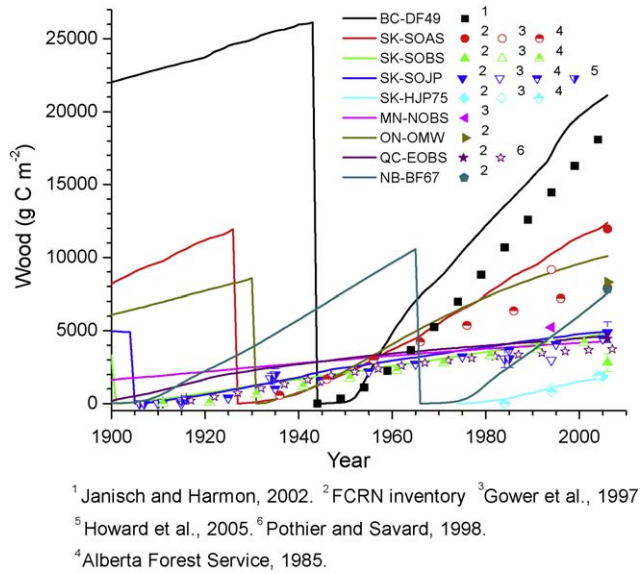

Fig. 12. Wood Alberta Forest Service, 1985; Gower et al., 1997; Janisch and Harmon, 2002; C modelled (lines) and measured or derived from measurements in various studies (symbols) at or near all FCRN flux tower sites with mature stands (see Table 1).

more rapid growth with warming in 2001 followed by slower growth with cooling and drying during the remainder of the 2001–2003 drought, and then more rapid growth with warming after 2004. Slower growth was apparent in both the aspen and jack pine tree ring chronologies during 2002–2004. Differences between gross and net growth in Fig. 11 were attributed to mortality, measured from annual tree death and modelled from annual mortality rates set in the model runs (see Section 2). At this stage of development, the model is not yet capable of simulating variable mortality rates caused by drought or pests, as apparent in the aspen tree-ring data. Variability in wood growth modelled at SK-SOJP was also similar to that of tree ring-width indices from jack pine in Ontario measured by Savva et al. (2008), who found slow growth in 1995–1996, followed by more rapid growth in 1998 and slower growth after 2000.

Wood C growth accumulated during the model runs at each FCRN site was compared with that derived from various inventory studies conducted at or near each site (Fig. 12). Large NEP (Fig. 9) drove more rapid wood growth at temperate coniferous BC-DF49 and NB-BF67 sites, intermediate NEP drove less rapid wood growth at the boreal deciduous SK-SOAS and mixed wood ON-OMW sites, and smaller NEP drove very slow wood growth at the boreal coniferous sites in SK, MB and QC.

4. Discussion

4.1. ENSO/PDO and NEP

The results presented here cover the entire period of flux tower operation at all mature FCRN sites from 1 January 1998 to 31 December 2006. Collectively these results indicate that continental-scale patterns of weather are reflected in those of NEP, although these patterns may vary with climate zone, species and topography. For example, ENSO warming events affected NEP differently at temperate coniferous and boreal deciduous forests (BC-DF49 in Fig. 2 *vs*. SK-SOAS in Fig. 3; also Fig. 8). Drought affected NEP differently at boreal deciduous and coniferous forests (SK-SOAS in Fig. 4 *vs*. SK-SOJP in Fig. 5) or at well- *vs*. poorly-drained boreal coniferous forests (SK-SOJP *vs*. SK-SOBS and MB-NOBS in Fig. 9).

Changes in NEP modelled and measured during and after the 1998/1999 ENSO/PDO event at BC-DF49 (Figs. 1, 9) appear to be part of a regional pattern. Falk et al. (2008) used EC to measure declines in annual NEP from the 1999 La Niña through the 2002/2003 El Niño over an old growth Douglas-fir/hemlock stand about 450 km south of BC-DF49, consistent with declines in annual NEP modelled at BC-DF49 from 1999 to 2004 (Fig. 9). Falk et al. (2008) attributed this decline to summer warming and drying, which was reversed by higher precipitation at their site in 2004. At a regional scale, Peterson and Peterson (2001) used tree-ring chronologies to infer that growth of low-elevation hemlock was negatively correlated with PDO warming during the 20th century in the U.S. Pacific Northwest, with a winter rainfall climate similar to that of BC-DF49.

The positive response of NEP to ENSO/PDO events modelled and measured at boreal sites such as SK-SOAS (e.g. Figs. 2 and 9) also appear to be part of a regional pattern. Peterson and Peterson (2001) found that growth of high elevation hemlock under cooler climates in the U.S. Pacific Northwest was positively correlated with PDO warming during the 20th century. Similarly, Pouliot et al. (2009) found that peak seasonal NDVIs of northern regions in Canada during 1985–2006 were more positively correlated with T_a while those of more southern regions were more negatively correlated. Zhou et al. (2001, 2003) also associated a general rise in NDVI in the northwestern boreal zone of North America with a rise in spring and summer T_a between 1982–1986 and 1995–1999, particularly in 1998. These associations were consistent with the higher NEP measured and modelled with warming in 1998 *vs*. 1999 and 2006 *vs*. 2004 at the boreal sites (Figs. 3, 6, 7 and 9). In Sweden, Lindroth et al. (2008) used EC measurements at two boreal spruce sites over 2 years to calculate rises in annual NEP with rises in mean annual temperature that were similar to those modelled and measured at the SK and NB sites from 2004 to 2006. Greater NEP in warmer years has been related to an extended duration of net C uptake at boreal deciduous sites in Canada (Barr et al., 2007) and at a range of deciduous and coniferous sites in Europe (Delpierre et al., 2009) as was measured and modelled at SK-SOAS (Figs. 3e and 6e), and at boreal coniferous sites as measured and modelled

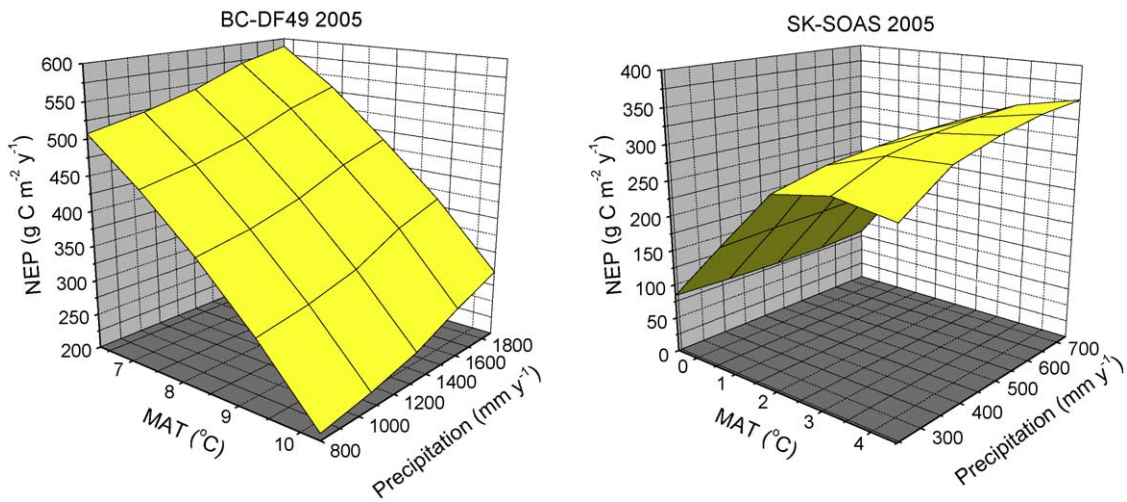

Fig. 13. Modelled response of NEP to changes in temperature and precipitation at BC-DF49 and SK-SOAS during 2005 following model spinup to the end of 2004.

elsewhere (Grant et al., 2008). However gains in NEP from extended C uptake with warming at coniferous sites were limited by adverse effects of higher T_a on net CO_2 exchange during summer (Figs. 2c, 5c and 8). These gains may therefore be smaller than those at deciduous sites (e.g. 2004–2006 in Fig. 9) where such adverse effects were less apparent (Fig. 4c).

The net effect of warming/cooling during ENSO/PDO events on terrestrial C exchange therefore depends upon the relative magnitudes and areas of contrasting changes in NEP under boreal *vs*. temperate climates. The net effect of these events on terrestrial C exchange is also determined by the greater incidence of fire (e.g. Jones and Cox, 2005) and mortality (Clark, 2004) with warming, especially in South America and SE Asia. The 1998/1999 PDO/ENSO event coincided with a larger increase of C_a in 1998 followed by a smaller increase in 1999 (Prentice et al., 2001), suggesting that large-scale changes in NEP may have occurred within regions most affected by ENSO and PDO events.

4.2. Drought and NEP

Declines in NEP measured and modelled at several boreal sites during the 2001–2003 drought (Figs. 4, 5 and 9) varied with topography and precipitation, but were part of a continental pattern. This drought caused widespread declines in growth of aspen (Hogg et al., 2008), jack pine (Metsaranta and Lieffers, 2009) (Fig. 11), and grassland (Grant and Flanagan, 2007) through much of mid-continental North America, and of agricultural and forest regions in Europe and Siberia (Ciais et al., 2005). These declines coincided with comparatively large increases in C_a (Jones and Cox, 2005), again suggesting large-scale declines in NEP within regions affected by this drought. Drought and high T_a most adversely affected net C uptake during July and August (Figs. 2c, 4c and 5c), consistent with trends towards increased C uptake in spring and reduced C uptake in summer under rising T_a at mid to high latitudes derived by Angert et al. (2005) from seasonal cycles of annually detrended C_a. Widespread declines in NEP (Fig. 9), LAI and NDVI (Fig. 10) during drier periods such as 2001–2003 may explain the declines in late-season photosynthetic activity in some continental boreal forests (e.g. Figs. 4e and 5e) inferred by Bunn and Goetz (2006) from temporally integrated MODIS NDVI over boreal North America between 1982 and 2003. Declines in NDVI under rising T_a were also reported in some North American boreal forest areas by Zhou et al. (2001). In both studies, these declines were attributed to temperature-induced drought, particularly in conifers as modelled here in Figs. 2c and 5c.

4.3. Sensitivity of modelled NEP to changes in temperature and precipitation

To study the contrasting effects of short-term changes in weather on annual NEP of a temperate coniferous and a boreal deciduous forest, the model runs for BC-DF49 and SK-SOAS in 2005 were repeated with step changes from recorded values of T_a and precipitation. This year's MAT was near-average at both sites, so that the step changes gave ranges of annual T_a and precipitation similar to those recorded at each site during the 1998–2006 experimental period (Table 2). Initial conditions for runs at each site (those at the end of 2004) were held constant to avoid carryover effects on NEP from differences in antecedent soil litter and water stocks. These step changes in T_a and precipitation were predicted by the model to cause large changes in annual NEP that spanned the range in values measured and modelled during 1998–2006 (Fig. 13). Rises in T_a lowered NEP at BC-DF49, and raised that at SK-SOAS particularly under higher precipitation, as modelled and measured at these sites in 1998 *vs*. 1999 (Figs. 2 and 3). Rises in precipitation raised annual NEP at BC-DF49 only slightly, and at SK-SOAS only under higher T_a. This rise in NEP with precipitation at SK-SOAS was limited by the larger water holding capacity of the soil at this site, and by greater than normal precipitation in 2004, which combined to delay the onset of water deficits under low precipitation in 2005. The response of NEP to precipitation modelled at SK-SOAS in 2005 would have been greater with drier antecedent conditions. These contrasting responses to warming indicate divergent changes in forest growth with interannual changes in weather, depending on forest type and climate zone. Such divergent changes are consistent with the complex changes in forest NDVI observed over time in several remote sensing studies (e.g. Bunn and Goetz, 2006; Goetz et al., 2005; Zhou et al., 2001, 2003). We should note that the changes in NEP modelled here represent responses to short-term changes in weather, and may differ from those modelled under long-term changes in climate during which changes in forest age, composition and nutrient cycling may also affect NEP.

4.4. Uncertainty of modelled and EC-derived NEP

Both modelled and EC-derived estimates of annual NEP (Fig. 9) were subject to some uncertainty which limited the constraint with which the modelled values could be tested. Uncertainty in modelled estimates may be caused by uncertainty in site conditions or in model parameters. Parameter values in *ecosys*

Table 4
Average contents of soil organic C (SOC) and variation in total soil N measured at SK-SOAS.

Horizon	L	F	H	Ae	Bt	Bmk	Ck1	Ck2
Depth to bottom (m)	0.02	0.05	0.10	0.32	0.70	0.85	1.25	1.85
Avg. SOC ($g\,kg^{-1}$)	430	415	313	6.56	3.96	2.46	2.62	1.08
Avg. total N ($g\,Mg^{-1}$)	20,199	21,573	19,522	469	330	205	226	47
Avg. total N + SD ($g\,Mg^{-1}$)	21,195	22,756	20,821	505	360	224	247	49
Avg. total N − SD ($g\,Mg^{-1}$)	19,293	20,507	18,376	438	305	189	208	45

Anderson (1998).

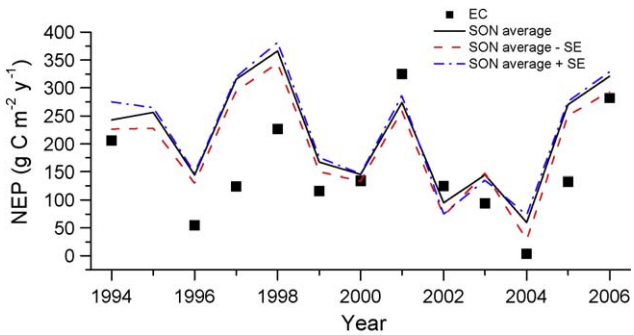

Fig. 14. Modelled response of NEP at SK-SOAS to changes in soil organic nitrogen (SON) when changed by ±1 SE from average values (see Table 4).

(e.g. Appendices A–C) are constrained by results from experiments conducted independently of the model and so are not changed for specific runs. However the model requires detailed inputs for site conditions, values of which may be uncertain due to spatial variation and sampling method. One key site input to which model results are sensitive is soil N and its ratio with soil organic C (SOC). This sensitivity was evaluated at SK-SOAS by estimating uncertainty in soil N from five profiles that had been sampled along a transect within the flux tower fetch. Standard deviations (SD) in soil C:N ratios of ±1 found in the horizons of these profiles were used to estimate a range of soil N that might accompany a given content of SOC (Table 4). Variation in annual NEP modelled at SK-SOAS from 1994 to 2006 with soil N in each horizon raised or lowered by one SD was ±15 $g\,C\,m^{-2}\,y^{-1}$ (Fig. 14).

Considerable effort has been directed towards estimating uncertainty in EC-derived estimates of annual NEP. Morgenstern et al. (2004) calculated a random variability of ±30 $g\,C\,m^{-2}\,y^{-1}$ in annual NEP estimated from EC measurements at BC-DF49 from 1998 to 2002. Griffis et al. (2003) calculated uncertainties of ±39 $g\,C\,m^{-2}\,y^{-1}$, 18 $g\,C\,m^{-2}\,y^{-1}$ and 15 $g\,C\,m^{-2}\,y^{-1}$ in EC-derived annual NEP in 2000 at SK-SOAS, SK-SOBS and SK-SOJP respectively. These uncertainties are comparable to those in modelled NEP caused by uncertainty in some key model inputs such as soil N.

Differences between modelled and EC-derived annual NEP exceeded these uncertainties at some FCRN sites (e.g. at ON-OMW and NB-BF67 in Fig. 9), although regressions of modelled *vs.* EC-measured CO_2 fluxes at these sites gave acceptable agreement (Table 2). These regressions are a stronger test of modelled values because they use hourly averages of 1/2-hourly EC flux measurements recorded under favourable site conditions, and exclude gap-filled values. In these cases, divergence between modelled and measured annual NEP may have arisen during the EC gap-filling process.

Acknowledgements

The Fluxnet-Canada Research Network is funded by the Natural Sciences and Engineering Research Council of Canada (NSERC), the Canadian Foundation for Climate and Atmospheric Sciences (CFCAS), and the Biological Implications of CO_2 Policy in Canada (BIOCAP). Computational facilities for *ecosys* were provided by the Westgrid high performance computing infrastructure. We thank Dr. Ted Hogg for the tree biomass data used in Fig. 11. The contributions of staff from the Department of Earth & Planetary Sciences, Harvard, and from the Department of Soil Science, University of Manitoba, for operating the MB-NOBS site in 2004–2005 and 2005–2006, respectively, are also gratefully acknowledged.

Appendix A. Supplementary data

Supplementary data associated with this article can be found, in the online version, at doi:10.1016/j.agrformet.2009.07.010.

References

Aakala, T., Kuuluvainen, T., De Grandpré, L., Gauthier, S., 2007. Trees dying standing in the northeastern boreal old-growth forests of Quebec: spatial patterns, rates, and temporal variation. Can. J. For. Res. 37, 50–61.
Alberta Forest Service, 1985. Alberta Phase 3 Forest Inventory: Yield Tables for Unmanaged Stands. Alberta Energy and Natl. Resour., Edmonton, Alberta.
Amthor, J.S., Chen, J.M., Clein, J., Frolking, S., Goulden, M.L., Grant, R.F., Kimball, J.S., King, A.W., McGuire, A.D., Nikolov, N.T., Potter, C.S., Wang, S., Wofsy, S.C., 2001. Boreal forest CO_2 exchange and evapotranspiration predicted by nine ecosystem process models: inter-model comparisons and relationships to field measurements. J. Geophys. Res. 106, 33623–33648.
Anderson, D., 1998. BOREAS TE-01 Soils Data over the SSA Tower Sites in Raster Format, Available online at http://www-eosdis.ornl.gov/ from the ORNL Distributed Active Archive Center, Oak Ridge National Laboratory, Oak Ridge, TN, U.S.A.
Angert, A., Biraud, S., Bonfils, C., Henning, C.C., Buermann, W., Pinzon, J., Tucker, C.J., Fung, I., 2005. Drier summers cancel out the CO_2 uptake enhancement induced by warmer springs. PNAS 102, 10823–10827.
Arain, M.A., Black, T.A., Barr, A.G., Jarvis, P.G., Massheder, J.M., Verseghy, D.L., Nesic, Z., 2002. Effects of seasonal and interannual climate variability on net ecosystem productivity of boreal deciduous and conifer forests. Can. J. For. Res. 32, 878–891.
Arain, M.A., Yuan, F., Black, T.A., 2006. Soil–plant nitrogen cycling modulated carbon exchanges in a western temperate conifer forest in Canada. Agric. For. Meteorol. 140, 171–192.
Barber, V.A., Juday, G.P., Finney, B.P., 2000. Reduced growth of Alaska white spruce in the twentieth century from temperature-induced drought stress. Nature 405, 668–673.
Barr, A.G., Black, T.A., Hogg, E.H., Kljun, N., Morgenstern, K., Nesic, Z., 2004. Inter-annual variability in the leaf area index of a boreal aspen-hazelnut forest in relation to net ecosystem production. Agric. For. Meteorol. 126, 237–255.
Barr, A.G., Black, T.A., Hogg, E.H., Griffis, T.J., Morgenstern, K., Kljun, N., Theede, A., Nesic, Z., 2007. Climatic controls on the carbon and water balances of a boreal aspen forest, 1994–2003. Global Change Biol. 13, 561–576.
Bergeron, O., Margolis, H.A., Black, T.A., Coursolle, C., Dunn, A.L., Barr, A.G., Wofsy, S.C., 2007. Comparison of carbon dioxide fluxes over three boreal black spruce forests in Canada. Global Change Biol. 13, 89–107.
Bonsal, B., Shabbar, A., 2008. Impacts of large-scale circulation variability on low streamflows over Canada: a review. Can. Water Resour. J. 33, 137–154.
Bonsal, B.R., Wheaton, E.E., 2005. Atmospheric circulation comparisons between the 2001 and 2002 and the 1961 and 1988 Canadian prairie droughts. Atmosphere-Ocean 43, 63–172.
Bonsal, B.R., Chakravarti, A.K., Lawford, R.G., 1993. Teleconnections between north Pacific SST anomalies and growing season extended dry spells on the Canadian Prairies. Int. J. Climatol. 13, 865–878.
Bonsal, B.R., Shabbar, A., Higuchi, K., 2001. Impacts of low frequency variability modes on Canadian winter temperature. Int. J. Climatol. 21, 95–108.
Brooks, J.R., Flanagan, L.B., Ehleringer, J.R., 1998. Responses of boreal conifers to climate fluctuations: indications from tree-ring widths and carbon isotope analyses. Can. J. For. Res. 28, 524–533.

Bunn, A., Goetz, S., 2006. Trends in satellite-observed circumpolar photosynthetic activity from 1982 to 2003: the influence of seasonality, cover type, and vegetation density. Earth Interact. 10, 1–19.
Churkina, G., Schimel, D., Braswell, B.H., Xiao, X., 2005. Spatial analysis of growing season length control over net ecosystem exchange. Global Change Biol. 11, 1777–1787.
Ciais, P., Reichstein, M., Viovy, N., Granier, A., Ogee, J., Allard, V., Aubinet, M., Buchmann, N., Bernhofer, C., Carrara, A., Chevallier, F., De Noblet, N., Friend, A.D., Friedlingstein, P., Grunwald, T., Heinesch, B., Keronen, P., Knohl, A., Krinner, G., Loustau, D., Manca, G., Matteucci, G., Miglietta, F., Ourcival, J.M., Papale, D., Pilegaard, K., Rambal, S., Seufert, G., Soussana, J.F., Sanz, M.J., Schulze, E.D., Vesala, T., Valentini, R., 2005. Europe-wide reduction in primary productivity caused by the heat and drought in 2003. Nature 437, 529–533.
Clark, D.A., 2004. Sources of Sinks? The responses of tropical forests to current and future climate and atmospheric composition. Philos. Trans. R. Soc. Lond. 359, 477–491.
Clark, D.A., Piper, S.C., Keeling, C.D., Clark, D.B., 2003. Tropical rain forest tree growth and atmospheric carbon dynamics linked to interannual temperature variation during 1984–2000. Proc. Natl. Acad. Sci. U.S.A. 100, 5852–5857.
D'Arrigo, R., Villalba, R., Wiles, G., 2001. Tree-ring estimates of Pacific decadal climate variability. Clim. Dyn. 18, 219–224, doi:10.1007/S003820100177.
Dang, Q.L., Lieffers, V.J., 1989. Climate and annual ring growth of black spruce in some Alberta peatlands. Can. J. Bot. 67, 1885–1889.
Delpierre, N., Soudani, K., François, C., Köstner, B., Pontailler, J.-Y., Nikinmaa, E., Misson, L., Aubinet, M., Bernhofer, C., Granier, A., Grünwald, T., Heinesch, B., Longdoz, B., Ourcival, J.-M., Rambal, S., Vesala, T., Dufrêne, E., 2009. Exceptional carbon uptake in European forests during the warm spring of 2007: a data-model analysis. Global Change Biol. 15, 1455–1474.
Dunn, A.L., Barford, C.C., Wofsy, S.C., Goulden, M.L., Daube, B.C., 2007. A long term record of carbon exchange in a boreal black spruce forest: means, responses to interannual variability, and decadal trends. Global Change Biol. 13, 577–590.
Falk, M., Wharton, S., Schroeder, M., Ustin, S., Paw, U.K.T., 2008. Flux partitioning in an old-growth forest: seasonal and interannual dynamics. Tree Physiol. 28, 509–520.
Fauria, M., Johnson, E.A., 2008. Climate and wildfires in the North American boreal forest. Philos. Trans. R. Soc. B 363, 2317–2329.
Gaumont-Guay, D., Black, T.A., Barr, A.G., Jassal, R.S., Nesic, Z., 2008. Biophysical controls on rhizospheric and heterotrophic components of soil respiration in a boreal black spruce stand. Tree Physiol. 28, 161–171.
Goetz, S.J., Bunn, A.G., Fiske, G.J., Houghton, R.A., 2005. Satellite-observed photosynthetic trends across boreal North America associated with climate and fire disturbance. PNAS 102, 13521–13525.
Gower, S.T., Vogel, J.G., Norman, J.M., Kucharik, C.J., Steele, S.J., Stow, T.K., 1997. Carbon distribution and aboveground net primary production in aspen, jack pine and black spruce stands in Saskatchewan and Manitoba, Canada. J. Geophys. Res. 102, 29,029–29,041.
Grant, R.F., Flanagan, L.B., 2007. Modeling stomatal and nonstomatal effects of water deficits on CO_2 fixation in a semiarid grassland. J. Geophys. Res. 112, G03011, doi:10.1029/2006JG000302.
Grant, R.F., Goulden, M.L., Wofsy, S.C., Berry, J.A., 2001a. Carbon and energy exchange by a black spruce–moss ecosystem under changing climate: testing the mathematical model ecosys with data from the BOREAS experiment. J. Geophys. Res. 106, 33605–33621.
Grant, R.F., Jarvis, P.G., Massheder, J.M., Hale, S.E., Moncrieff, J.B., Rayment, M., Scott, S.L., Berry, J.A., 2001b. Controls on carbon and energy exchange by a black spruce–moss ecosystem: testing the mathematical model ecosys with data from the BOREAS experiment Global Biogeochem. Cycles 15, 129–147.
Grant, R.F., Arain, A., Arora, V., Barr, A., Black, T.A., Chen, J., Wang, S., Yuan, F., Zhang, Y., 2005. Intercomparison of techniques to model high temperature effects on CO_2 and energy exchange in temperate and boreal coniferous forests. Ecol. Model. 188, 217–252.
Grant, R.F., Black, T.A., Gaumont-Guay, D., Kljun, N., Barr, A.G., Morgenstern, K., Nesic, Z., 2006a. Net ecosystem productivity of boreal aspen forests under drought and climate change: mathematical modelling with *ecosys*. FCRN Special Issue. Agric. For. Meteorol. 140, 152–170.
Grant, R.F., Zhang, Y., Yuan, F., Wang, S., Hanson, P.J., Gaumont-Guay, D., Chen, J., Black, T.A., Barr, A., Baldocchi, D.D., Arain, A., 2006b. Intercomparison of techniques to model water stress effects on CO_2 and energy exchange in temperate and boreal deciduous forests. Ecol. Model. 196, 289–312.
Grant, R.F., Barr, A.G., Black, T.A., Iwashita, I., Kidson, J., McCaughey, H., Morgenstern, K., Murayama, S., Nesic, Z., Saigusa, N., Shashkov, A., Zha, T., 2007a. Net ecosystem productivity of boreal jack pine stands regenerating from clearcutting under current and future climates. Global Change Biol. 13, 1423–1440.
Grant, R.F., Black, T.A., Humphreys, E.R., Morgenstern, K., 2007b. Changes in net ecosystem productivity with forest age following clearcutting of a coastal Douglas fir forest: testing a mathematical model with eddy covariance measurements along a forest chronosequence. Tree Physiol. 27, 115–131.
Grant, R.F., Margolis, H.A., Barr, A.G., Black, T.A., Dunn, A.L., Bernier, P.Y., Bergeron, O., 2008. Changes in net ecosystem productivity of boreal black spruce stands in response to changes in temperature at diurnal and seasonal time scales. Tree Physiol. 29, 1–17.
Griffis, T.J., Black, T.A., Morgenstern, K., Barr, A.G., Nesic, Z., Drewitt, G.B., Gaumont-Guay, D., McCaughey, J.H., 2003. Ecophysiological controls on the carbon balances of three southern boreal forests. Agric. For. Meteorol. 117, 53–71.
Hassan, Q.K., Bourque, C.P.-A., Meng, F.-R., 2006. Estimation of daytime net CO_2 exchange over balsam fir forests in eastern Canada: combining averaged tower-based flux measurements with remotely sensed MODIS data. Can. J. Remote Sens. 32, 405–416.
Hogg, E.H., Brandt, J.P., Michaelian, M., 2008. Impacts of a regional drought on the productivity, dieback and biomass of western Canadian aspen forests. Can. J. For. Res. 38, 1373–1384.
Holland, E.A., Dentener, F.J., Braswell, B.H., Sulzman, J.M., 1999. Contemporary and pre-industrial global reactive nitrogen budgets. Biogeochemistry 46, 7–43.
Howard, E.A., Gower, S.T., Foley, J.A., Kucharik, C.J., 2004. Effects of logging on carbon dynamics of a jack pine forest in Saskatchewan, Canada. Global Change Biol. 10, 1–18.
Janisch, J.E., Harmon, M.E., 2002. Successional changes in live and dead wood carbon stores: implications for net ecosystem productivity. Tree Physiol. 22, 77–89.
Jassal, R.S., Black, T.A., Cai, T., Morgenstern, K., Li, Z., Gaumont-Guay, D., Nesic, Z., 2007. Components of ecosystem respiration and an estimate of net primary productivity of an intermediate-aged Douglas-fir stand. Agric. For. Meteorol. 144, 44–57.
Jones, C.D., Cox, P.M., 2005. On the significance of atmospheric CO_2 growth rate anomalies in 2002–2003. Geophys. Res. Lett. 32, L14816, doi:10.1029/2005GL023027.
Jump, A.S., Hunt, J.M., Peñuelas, J., 2006. Rapid climate change-related growth decline at the southern range edge of *Fagus sylvatica*. Global Change Biol. 12, 2163–2174.
Keeling, R.F., Piper, S.C., Heimann, M., 1996. Global and hemispheric CO_2 sinks deduced from changes in atmospheric O_2 concentration. Nature 381, 218–221.
Kling, G.W., Kipphut, G.W., Miller, M.C., 1991. Arctic lakes and streams as gas conduits to the atmosphere: implications for tundra carbon budgets. Science 251, 298–301.
Kljun, N., Black, T.A., Griffis, T.J., Barr, A.G., Gaumont-Guay, D., Morgenstern, K., McCaughey, J.H., Nesic, Z., 2007. Response of net ecosystem productivity of three boreal forest stands to drought. Ecosystems 10, 1039–1055.
Krishnan, P., Black, T.A., Grant, N.J., Barr, A.G., Hogg, E.H., Jassal, R.S., Morgenstern, K., 2006. Impact of changing soil moisture distribution on net ecosystem productivity of a boreal aspen forest during and following drought. Agric. For. Meteorol. 139, 208–223.
Krishnan, P., Black, T.A., Barr, A.G., Grant, N.J., Gaumont-Guay, D., Nesic, Z., 2008. Factors controlling the interannual variability in the carbon balance of a southern boreal black spruce forest. J. Geophys. Res. 113, D09109, doi:10.1029/2007JD008965.
Larsen, C.P.S., MacDonald, G.M., 1995. Relations between tree-ring widths, climate, and annual area burned in the boreal forest of Alberta. Can. J. For. Res. 25, 1746–1755.
Le Goff, H., Flannigan, M.D., Bergeron, Y., Girardin, M.P., 2007. Historical fire regime shifts related to climate teleconnections in the Waswanipi area, central Quebec, Canada. Int. J. Wildland Fire 16, 607–618.
Lindroth, A., Klemedtsson, L., Grelle, A., Weslien, P., Langvall, O., 2008. Measurement of net ecosystem exchange, productivity and respiration in three spruce forests in Sweden shows unexpectedly large soil carbon losses. Biogeochemistry 89, 43–60.
Luyssaert, S., Janssens, I.A., Sulkava, M., Papale, D., Dolman, A.J., Reichstein, M., Hollmén, J., Martin, J.G., Suni, T., Vesala, T., Loustau, D., Law, B.E., Moors, E.J., 2007. Photosynthesis drives anomalies in net carbon-exchange of pine forests at different latitudes. Global Change Biol. 13, 2110–2127.
McCaughey, J.H., Pejam, M.R., Arain, M.A., Cameron, D.A., 2006. Carbon dioxide and energy fluxes from a boreal mixedwood forest ecosystem in Ontario, Canada. Agric. For. Meteorol. 140, 79–96.
Meteorological Service of Canada, 2004. Canadian acid deposition science assessment. Environment Canada, Ottawa, ON.
Metsaranta, J.M., Lieffers, V.J., 2009. Using dendrochronology to obtain annual data for modelling stand development: a supplement to permanent sample plots. Forestry 82, 163–173.
Morgenstern, K., Black, T.A., Humphreys, E.R., Griffis, T.J., Drewitt, G.B., Cai, T., Nesic, Z., Spittlehouse, D.L., Livingstone, N.J., 2004. Sensitivity and uncertainty in the carbon balance of a Pacific northwest Douglas fir forest during an El Niño/El Niña cycle. Agric. For. Meteorol. 123, 201–219.
Myneni, R.B., Keeling, C.D., Tucker, C.J., Asrar, G., Nemani, R.R., 1997. Increased plant growth in the northern high latitudes from 1981 to 1991. Nature 386, 698–702.
Nabuurs, G.J., Pussinen, A., Karjalainen, T., Erhard, M., Kramer, K., 2002. Stemwood volume increment changes in European forests due to climate change: a simulation study with the EFISCEN model. Global Change Biol. 8, 304–316.
Nemani, R.R., Keeling, C.D., Hashimoto, H., Jolly, W.M., Piper, S.C., Tucker, C.J., Myneni, R.B., Running, S.W., 2003. Climate-driven increases in global terrestrial net primary production from 1982 to 1999. Science 300, 1560–1563.
Peterson, D.W., Peterson, D.L., 2001. Mountain hemlock growth responds to climatic variability at annual and decadal time scales. Ecology 82, 3330–3345.
Piao, S., Ciais, P., Friedlingstein, P., Peylin, P., Reichstein, M., Luyssaert, S., Margolis, H., Fang, J.Y., Barr, A., Chen, A.P., Grelle, A., Hollinger, D.Y., Laurila, T., Lindroth, A., Richardson, A.D., Vesala, T., 2008. Net carbon dioxide losses of northern ecosystems in response to autumn warming. Nature 451, 49–52.
Pothier, D., Savard, F., 1998. Actualisation des tables de production pour les principales espèces forestières du Québec. Ministère des Ressources Naturelles du Québec, 183 pp.
Pouliot, D., Latifovic, R., Olthof, I., 2009. Trends in vegetation NDVI from 1 km AVHRR data over Canada for the period 1985-2006. Int. J. Remote Sens. 30, 149–168.
Prentice, I.C., Farquhar, G.D., Fasham, M.J.R., Goulden, M.L., Heimann, M., Jaramillo, V.J., Kheshgi, H.S., Le Quéré, C., Scholes, R.J., Wallace, D.W.R., 2001. The carbon

cycle and atmospheric carbon dioxide. In: Houghton, J.T., et al. (Eds.), Climate Change 2001: The Scientific Basis. Cambridge University Press, Cambridge, pp. 183–238.

Richardson, A.D., Hollinger, D.Y., Burba, G.G., Davis, K.J., Flanagan, L.B., Katul, G.G., Munger, J.W., Ricciuto, D.M., Stoy, P.C., Suyker, A.E., Verma, S.B., Wofsy, S.C., 2006. A multi-site analysis of random error in tower-based measurements of carbon and energy fluxes. Agric. For. Meteorol. 136, 1–18.

Richey, J.E., Melack, J.M., Aufdenkampe, A.K., Ballester, V.M., Hess, L.M., 2002. Outgassing from Amazon rivers and wetlands as a large tropical source of atmospheric CO_2. Nature 416, 617–620.

Rosenzweig, C., Casassa, G., Karoly, D.J., Imeson, A., Liu, C., Menzel, A., Rawlins, S., Root, T.L., Seguin, B., Tryjanowski, P., 2007. Assessment of observed changes and responses in natural and managed systems. In: Parry, M.L., Canziani, O.F., Palutikof, J.P., van der Linden, P.J., Hanson, C.E. (Eds.), Climate Change 2007: Impacts, Adaptation and Vulnerability. Contribution of Working Group II to the Fourth Assessment Report of the Intergovernmental Panel on Climate Change. Cambridge University Press, Cambridge, UK, pp. 79–131.

Saleska, S.R., Miller, S.D., Matross, D.M., Goulden, M.L., Wofsy, S.C., da Rocha, H.R., de Camargo, P.B., Crill, P., Daube, B.C., de Freitas, H.C., Hutyra, L., Keller, M., Kirchhoff, M., Menton, M., Munger, J.W., Pyle, E.H., Rice, A.H., Silva, H., 2003. Carbon in Amazon forests: unexpected seasonal fluxes and disturbance-induced losses. Science 302, 1554–1557.

Savva, Y., Bergeron, Y., Denneler, B., Koubaa, A., Tremblay, F., 2008. Effect of interannual climate variations on radial growth of jack pine provenances in Petawawa, Ontario. Can. J. For. Res. 38, 619–630.

Shabbar, A., Skinner, W., 2004. Summer drought patterns in Canada and the relationships to global sea surface temperatures. J. Clim. 17, 2866–2880.

Skinner, W.R., Shabbar, A., Flannigan, M.D., Logan, K., 2006. Large forest fires in Canada and the relationship to global sea surface temperatures. J. Geophys. Res. 111, D14106, doi:10.1029/2005JD006738.

Welp, L.R., Randerson, J.T., Liu, H.P., 2007. The sensitivity of carbon fluxes to spring warming and summer drought depends on plant functional type in boreal forest ecosystems. Agric. For. Meteorol. 147, 172–185.

Wesely, M.L., Hart, R.L., 1985. Variability of short term eddy-correlation estimates of mass exchange. In: Hutchinson, B.A., Hicks, B.B. (Eds.), The forest–atmosphere interaction. D. Reidel, Dordrecht, pp. 591–612.

Wilmking, M., Juday, G.P., Barber, V.A., Zald, H.J., 2004. Recent climate warming forces contrasting growth responses of white spruce at treeline in Alaska through temperature thresholds. Global Change Biol. 10, 1724–1736.

Yuan, F., Arain, M.A., Barr, A.G., Black, T.A., Bourque, C.P.A., Coursolle, C.E., Margolis, H.A., McCaughey, J.H., Wofsy, S.C., 2008. Modeling analysis of primary controls on net ecosystem productivity of seven boreal and temperate coniferous forests across a continental transect. Global Change Biol. 14, 1765–1784.

Zhou, L., Tucker, C.J., Kaufmann, R.K., Slayback, D., Shabanov, N.V., Myneni, R.B., 2001. Variations in northern vegetation activity inferred from satellite data of vegetation index during 1981 to 1999. J. Geophys. Res. 106, 20,069–20,083.

Zhou, L., Kaufmann, R., Tian, Y., Myneni, R., Tucker, C., 2003. Relation between interannual variations in satellite measures of northern forest greenness and climate between 1982 and 1999. J. Geophys. Res. 108, 1–11.